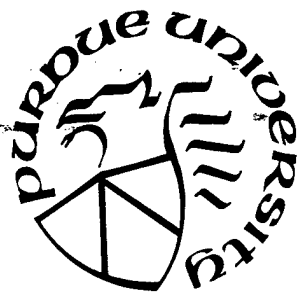# RAY W. HERRICK LABORATORIES

A Graduate Research Facility
of The School of Mechanical Engineering

PERFORMANCE OF STRAIGHT-FIN AND
MICROCHANNEL HEAT EXCHANGERS IN
STEADY AND PERIODIC FLOWS

Purdue University

West Lafayette, Indiana 47907-1077

PERFORMANCE OF STRAIGHT-FIN AND MICROCHANNEL HEAT EXCHANGERS IN STEADY AND PERIODIC FLOWS

Sponsored by
Office of Naval Research

HL 2001-18   Report #1614-1

Submitted by: Aaron Alexander, Graduate Research Assistant
                   Luc Mongeau, Co-Principal Investigator
                   James Braun, Co-Principal Investigator

Approved by: Robert J. Bernhard, Director
                   Ray W. Herrick Laboratories

OCTOBER 2001

20011018 038

_

REPORT DOCUMENTATION PAGE

Form Approved
OMB No. 0704-0188

Public reporting burden for this collection of information is estimated to average 1 hour per response, including the time for reviewing instructions, searching data sources, gathering and maintaining the data needed, and completing and reviewing the collection of information. Send comments regarding this burden estimate or any other aspect of this collection of information, including suggestions for reducing this burden to Washington Headquarters Service, Directorate for Information Operations and Reports, 1215 Jefferson Davis Highway, Suite 1204, Arlington, VA 22202-4302, and to the Office of Management and Budget, Paperwork Reduction Project (0704-0188) Washington, DC 20503.

PLEASE DO NOT RETURN YOUR FORM TO THE ABOVE ADDRESS.

1. REPORT DATE *(DD-MM-YYYY)*	2. REPORT DATE	3. DATES COVERED *(From - To)*
08-10-2001	Final Report	May 1999 – May 2001

4. TITLE AND SUBTITLE	5a. CONTRACT NUMBER
PERFORMANCE OF STRAIGHT-FIN AND MICROCHANNEL HEAT EXCHANGERS IN STEADY AND PERIODIC FLOWS	**5b. GRANT NUMBER** N00014-99-10642
	5c. PROGRAM ELEMENT NUMBER PE 61153N

6. AUTHOR(S)	5d. PROJECT NUMBER
Alexander, Aaron	
Mongeau, Luc	**5e. TASK NUMBER**
Braun, James E.	
	5f. WORK UNIT NUMBER

7. PERFORMING ORGANIZATION NAME(S) AND ADDRESS(ES)	8. PERFORMING ORGANIZATION REPORT NUMBER
Purdue Research Foundation Division of Sponsored Programs Hovde Hall, Third Floor West Lafayette, IN 47907	HL2001-18

9. SPONSORING/MONITORING AGENCY NAME(S) AND ADDRESS(ES)	10. SPONSOR/MONITOR'S ACRONYM(S)
Office of Naval Research, ONT 331 Ballston Centre Tower One 800 North Quincy Street Arlington, VA 22217-5600	
	11. SPONSORING/MONITORING AGENCY REPORT NUMBER

12. DISTRIBUTION AVAILABILITY STATEMENT

Approved for public release: distribution unlimited

13. SUPPLEMENTARY NOTES

14. ABSTRACT

The performance of straight-fin and microchannel heat exchangers was investigated in steady and periodic flows. Steady flow measurements were performed using an open test section wind tunnel. Periodic flow measurements were performed using a thermoacoustic cooler prototype. Detailed temperature measurements were made for varying operating conditions using thermocouple arrays. The results suggest that nondimensional heat transfer coefficients based on stack end temperatures calculated from steady flow data may be applicable to predict the thermal performance in a periodic flow, provided the root-mean-square local particle velocity is used as the velocity scale. The accuracy of rms-based steady flow correlations may be comparable or in some cases better than that of linearized boundary layer models frequently used in thermoacoustics.

15. SUBJECT TERMS

Heat exchangers, thermoacoustics

16. SECURITY CLASSIFICATION OF:			17. LIMITATION OF ABSTRACT	18. NUMBER OF PAGES	19a. NAME OF RESPONSIBLE PERSON
a. REPORT	b. ABSTRACT	c. THIS PAGE			
U	U	U	UU	53	**19b. TELEPONE NUMBER** *(Include area code)*

Standard Form 298 (Rev. 8-98)
Prescribed by ANSI-Std Z39-18

TABLE OF CONTENTS

LIST OF FIGURES

NOMENCLATURE

English Symbols

A_f = entire fin surface area, (m^2)

A = total heat exchanger surface area, $A = A_t + A_f$ (m^2)

A_{fc} = fin cross-sectional area, $A_{fc} = wt$, (m^2)

A_o = external total surface area, (m^2)

A_c = flow area(air side flow), (m^2)

A_{cs} = tube internal cross sectional area (m^2)

A_t = entire tube external surface area (m^2)

A_i = tube internal surface area, $A_i = \pi D_i L_t$, (m^2)

c_p = constant pressure specific heat, (J/kg-K)

D_h = hydraulic diameter (air-side flow), $D_h = \dfrac{4LA_c}{A}$, (m)

D_i = secondary flow tube inside diameter, (m)

D_o = secondary flow tube outside diameter, (m)

f_G = friction factor for flow in smooth tubes, $f_G = (.79 \ln Re_D - 1.64)^{-2}$

Gz = Graetz number, $Gz = \dfrac{Re_D Pr_{sf}}{(L/Di)}$

h = heat transfer coefficient, (W/m^2-K)

h_i = internal flow heat transfer coefficient, (W/m^2-K)

h_o = external flow heat transfer coefficient, (W/m^2-K)

j = j-Colburn factor, dimensionless heat transfer coefficient, $j = St\, Pr^{2/3}$

6

k = thermal conductivity, (W/m-K)

k_{sf}= thermal conductivity of secondary fluid, (W/m-K)

L= fin length, length of flow path of interest, (m)

LMTD = log mean temperature difference, (K)

L_t=total tube length, (m)

$\dot{m}$ = mass flow rate, (kg/s)

$$m^2 = \frac{hP}{kA_c}, \ (m^{-2})$$

Nt=number of tubes in exchanger

Nu = Nusselt number, $\ Nu = \dfrac{hD}{k}$

P = perimeter, $\ P = 2w + 2t$, (m)

Pr = Prandtl number, $\ Pr = \dfrac{c_p \mu}{k}$

$\dot{Q}$ = heat transfer rate, (W)

R = radius of heat exchanger viewed by flow, (m)

$R_{c,i}$ = secondary tube internal convective resistance, (K/W)

Re = Reynolds number, $\ Re = \dfrac{uL\rho}{\mu}$

R_{fins} = combined fin conductive and convective resistance, (K/W)

$R_{p,t}$ = convective resistance between secondary tube wall and primary fluid, (K/W)

R_{tw} = secondary tube wall conductive resistance, (K/W)

S_l = tube spacing in the air flow direction, (m)

St = Stanton number, $\ St = \dfrac{Nu}{Re\,Pr}$

S_t = tube spacing normal to the flow, (m)

s = spacing between adjacent fins, (m)

T = temperature, (K)

TS=distance between tube centerlines, (m)

t = fin thickness, (m)

t_t= tube height (microchannel heat exchanger), (m)

UA = overall system heat transfer coefficient, (W/K)

w = fin depth in direction of flow, (m)

w_t= tube width (microchannel heat exchanger), (m)

Greek Symbols

$$\alpha = \text{thermal diffusivity} = \frac{k}{\rho c_p}, \text{ (m}^2\text{/s)}$$

δ_t = thermal penetration depth, (m)

$$\eta_o = \text{ overall fin efficiency}, \eta_o = 1 - \frac{A_f}{A}(1 - \eta_f)$$

$$\eta_f = \text{ single fin efficiency}, \eta_f = \frac{\tanh(mL)}{mL} \text{ (for straight or pin fin)}$$

μ = dynamic viscosity, $(N \cdot s/m^2)$

ω = frequency, Hz.

Subcripts

h = hot

c = cold, convective

i = in, internal

o = out, outer

t = tube

tw = tube wall

sf = secondary fluid

s = surface

fc = fin cross-section

1.0 Introduction

Thermoacoustic cooling involves heat transfer between gas particles within high amplitude acoustic standing waves and heat exchangers immersed into the working gas. The dynamic pressure and velocity changes inherent in an acoustic wave cause a net flow of heat up a mean temperature gradient along the direction of sound wave propagation.

The so-called thermoacoustic refrigeration cycle describes the heat transfer process within the working gas, which is comparable to a reverse Brayton cycle. Thermoacoustic heat pumping systems include a porous substrate called a stack, which enhances the heat flux within the working gas. Heat is rejected to and pumped from hot and cold heat exchangers, which are usually fin-tube and are generally placed on each end of the stack. The cold heat exchanger provides heat to the working gas removing it from the secondary fluid that flows through the heat exchanger channels. Conversely, the hot heat exchanger removes heat from the working gas and rejects it into another secondary fluid loop (Swift, 1999).

Thermoacoustic particle displacement amplitudes are typically between 1 and 10 mm, and the operating temperature differences between the working gas and the secondary fluid are relatively small (< 5 °C). Proper design and sizing of the heat exchanger is of paramount importance. This includes proper fin spacing, tube design, tube spacing, and fin stream wise depth.

In order to predict the performance of heat exchangers at the design stage, before implementation in a working system, analytical or semi-empirical models are necessary. These models must account for the fact that there is no forced mean flow, and oscillatory gas pulsations are present within the thermoacoustic environment. It is necessary to estimate heat transfer coefficients for oscillating flow conditions.

Most heat exchanger models reported in the literature assume steady flow conditions in the primary working fluid. Currently, there are very few tools for predicting heat transfer in oscillating flows. Mozurkewich (1995,1998a, 1998b, 2000) has developed numerical prediction tools for thermoacoustic design. Additionally, he has conducted experiments on thermoacoustic heat transfer from a cylinder, and from transverse tubes in pulsatile flow. He found that for large acoustic velocity, the heat transfer in acoustically driven flow can be approximated by a time-averaged laminar steady flow correlation. Swift (1992, 1999) has also conducted many analytical and experimental studies of thermoacoustic phoenomena, including thermoacoustic heat transfer this general area in which he was also looking to better predict thermoacoustic heat transfer for design. In his thermoacoustic handbook (1999), the general ideas for various heat exchangers used in thermoacoustic devices are given. There have been a few other noteworthy contributions to this field, including Wetzel (1999, 2000) who studied the effect of heat transfer from a single plate and Brewster (1997) who studied the effects of heat transfer between the elements in a thermoacoustic system. Yet, very few experimental studies for actual heat exchangers in-situ have been conducted. Mozurkewich's experiment was done using a wire in a tube and Wetzel's was done with a single plate. Their results cannot be directly applied to find a correlation in oscillating flow in real thermoacoustic systems due to the different geometry. Therefore, experiments for real heat exchangers are valueable and should be done. The objectives of the work presented in this report were to develop methods for predicting the performance of heat exchangers in an oscillating flow environment, and to investigate the performance of microchannel heat exchangers. In order to accomplish these goals, both steady and oscillating flow tests were performed for one conventional fin-tube and one microchannel heat exchanger. The fin-tube heat exchanger was designed, built, and installed in a thermoacoustic prototype

designed for a low-capacity air-conditioning application in a previous study (Minner et al., 2000). The microchannel heat exchanger was designed and built specifically for the purpose of this study. Both heat exchangers were installed in similar flanges, which facilitated their installation in the thermoacoustic system. The existing thermoacoustic prototype was used as the environment for testing the heat exchangers in an oscillating flow. A small-scale wind tunnel was also developed for testing the steady flow performance of both heat exchangers.

There were several reasons for performing steady flow tests, including: 1) establishing procedures for estimating heat transfer coefficients from measurements and for correlating heat transfer coefficients with dimensionless parameters, 2) providing baseline data for comparing the performance of the different heat exchangers under identical flow conditions, and 3) validating theoretical steady flow heat transfer coefficient correlations that could be adapted for use in estimating heat transfer coefficients for oscillating flow environments.

For oscillating flows, special procedures were established for estimating heat transfer coefficients from measured data and for correlating the heat transfer coefficients with dimensionless parameters. Heat exchanger specific correlations are appropriate for use in system simulations. However, they are not useful in predicting the effects of heat exchanger design changes. For this purpose, two different approaches were investigated for estimating heat transfer coefficients using design parameters. One approach involves a theoretical calculation of conduction across a laminar boundary layer that is used in the DeltaE computer program (Ward 1993). The second approach involves adapting existing steady flow heat transfer correlations to oscillating flow environments.

2.0 Heat Exchanger Descriptions

Two different heat exchangers were investigated in this study. Firstly, a conventional fin-tube heat exchanger was used for preliminary studies and to develop accurate measurement procedures. Secondly, a microchannel heat exchanger, designed and built specifically for this project, was tested. In the context of this study, a microchannel heat exchanger is defined as a heat exchanger with small primary fluid pore spacing and thin (normal to the flow direction) secondary fluid tubing. A detailed description of both heat exchangers follows.

2.1 Straight Plate Finned-Tube Heat Exchanger

A straight plate fin-tube heat exchanger was built by a commercial manufacturer and is depicted in figures 1and 2 along with relevant dimensions. This heat exchanger was part of a set of two heat exchangers designed and built for a thermoacoustic prototype. Due to manufacturing constraints, it was necessary to make several compromises in the design. In particular, the stream wise depth was several times larger than the acoustic particle displacement associated with the thermoacoustic prototype. It has been reported that depths on the order of the particle displacement length are preferable (Swift, 1999). Furthermore, the width and spacing of the fins were not optimal according to guidelines established in previous design optimization studies (Minner, 1996).
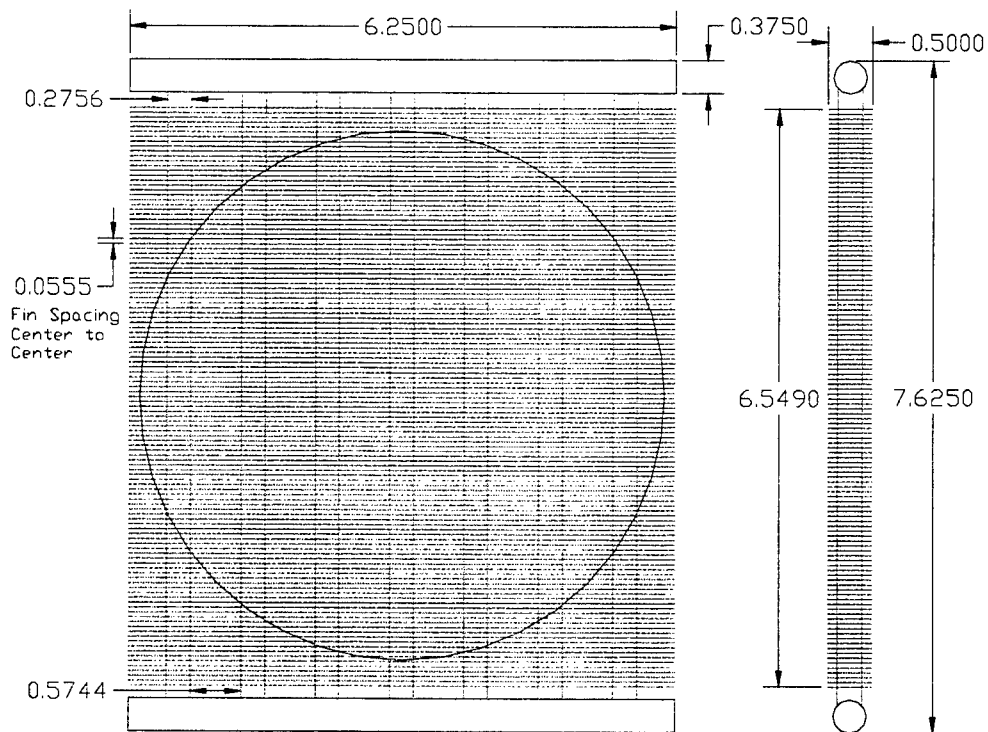
Figure 1: *Drawing of Fin-tube Heat Exchanger (dimenions in inches)*
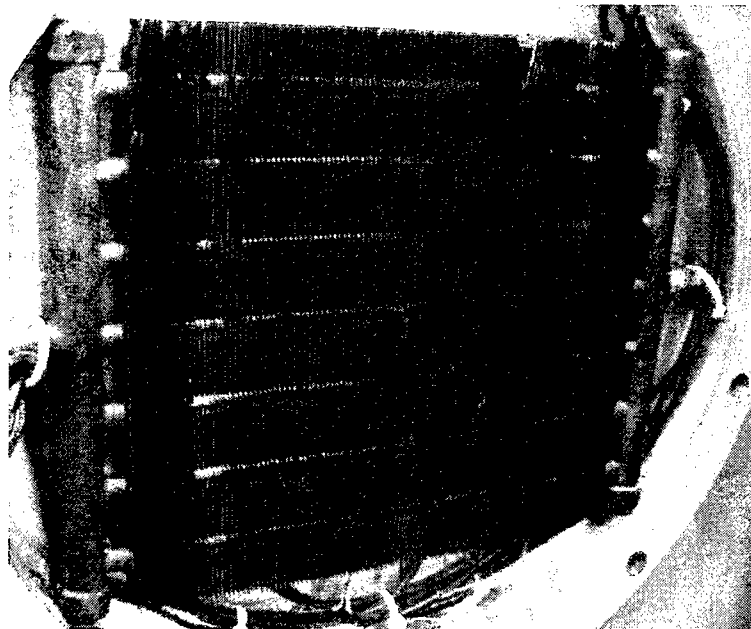
Figure 2: *Picture of Installed Fin-Tube Heat Exchanger*

14

2.2 Microchannel Heat Exchanger

Figures 3 and 4 depict the microchannel heat exchanger. Several advantageous features distinguish this design from that of the conventional fin-tube design shown in figure 1. Firstly, the use of small rectangular flow channels for the secondary fluid presents a smaller obstruction to the flow of the primary thermoacoustic working fluid for a given tube surface area. Secondly, the use of the microchannel and two-pass secondary flow geometry leads to higher secondary fluid heat transfer coefficients. Thirdly, the microchannel design incorporates outer fins having a smaller depth, tighter spacing, and larger overall surface area.
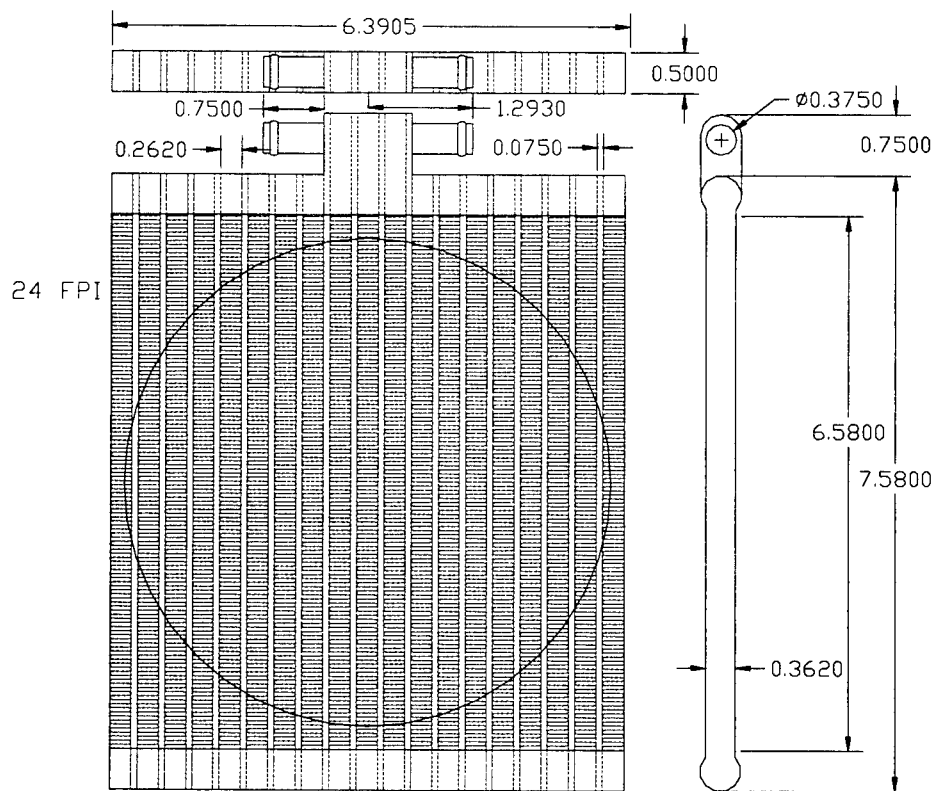
Figure 3: Drawing of Microchannel Heat Exchanger (dimensions in inches)
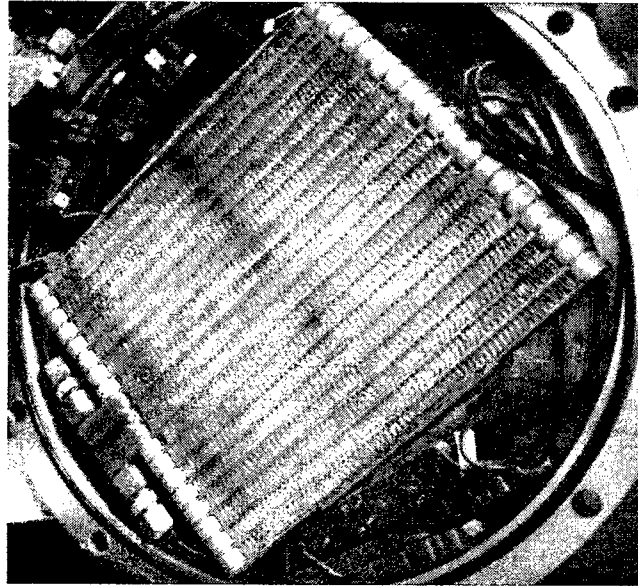
Figure 4: Picture of Installed Microchannel Heat Exchanger

3.0 Experimental Apparatus

3.1 Wind Tunnel for steady flow measurements

A small-scale wind tunnel was designed and built to perform measurements necessary for

estimating air-side heat transfer coefficients. The heat exchangers were operated at steady state

in a steady flow with water flowing through the tubes. The wind tunnel, shown in figures 5 and

6, consisted of a centrifugal fan powered by a Baldor Electric Motor (Model M3115) and a 15

cm (6 in) diameter PVC pipe. A flow straightener was used to minimize inflow swirl and

transverse flow motion. An inlet bell mouth and a plenum settling chamber downstream of the

heat exchangers were utilized to improve the flow velocity profile uniformity across the duct.

The heat exchanger was mounted between two sections of PVC pipe. A pitot tube, in

conjunction with a probe traversing mechanism and a Dwyer inclined manometer (Model

number 115-AV), was used to measure the airflow velocity distribution across the pipe at one

stream wise location. The velocity distribution was used to determine the air mass flow rate.
Hot water flow rates through the heat exchanger were measured using an axial paddle wheel
turbine type flow meter (JLC International IR-Opflow Type 4) at the water outlet.
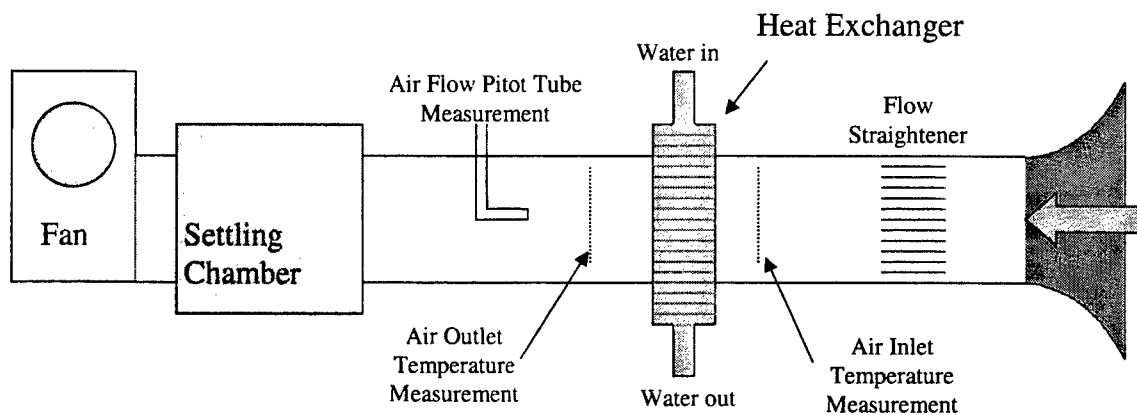
Figure 5: Schematic of the Wind Tunnel used for the Steady Flow Measurements.
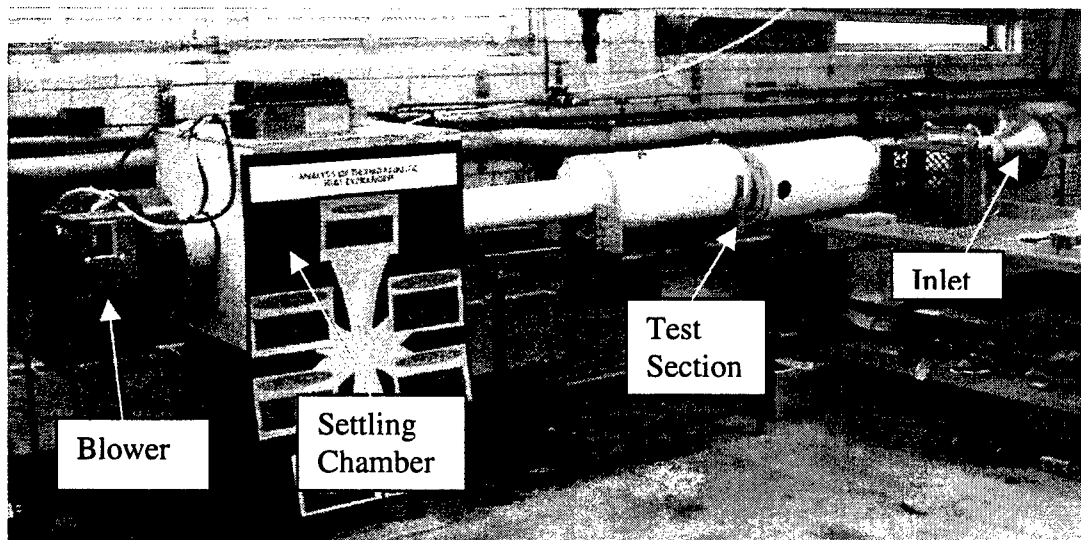
Figure 6: Picture of the Wind Tunnel used for the Steady Flow Measurements.

A differential temperature transducer (Delta-T Company, Model number 75X) was used
to measure the water temperature difference. At the inlet and the outlet of the wind tunnel,

17

arrays of type T thermocouples (N=9) were installed, at the locations shown in figure 5 to measure air temperatures. The rate of heat transfer was calculated from the measured flow rates and temperatures for both the air-side and the water-side of the exchanger, as described in section 5.

3.2 Thermoacoustic System for Unsteady Flow Measurements

Unsteady heat exchanger performance measurements were made using a functional thermoacoustic cooler. The thermoacoustic cooler was designed and built at Purdue University (Minner et al., 2000). The schematic of the thermoacoustic cooler is shown in figure 7 and the picture of the experimental setup is shown in figure 8. It is driven by a 300 W moving magnet linear actuator mounted on metal "leaf" springs to provide suspension stiffness. Type T thermocouples were used to perform detailed temperature measurements at several locations on the heat exchangers. The driver was instrumented with an accelerometer on the driver piston. A pressure sensor was installed in a port near the piston. These dynamic pressure and velocity measurements at the piston face were used as inputs to DELTAE (Ward, 1993) to estimate the root-mean-square (rms) velocity within each heat exchanger. This velocity was used to determine acoustic Reynolds numbers in an attempt to correlate heat transfer data for periodic flows and to compare them with steady flow heat transfer coefficients, as described in greater detail in the next section.

The device was operated with two heat exchangers and a stack producing a temperature difference between the circulating water stream and the thermoacoustic working fluid at each heat exchanger. The stack was composed of a 76 μm thick polyester film and 254 μm thick nylon wire constructed by using the wire as a spacer and rolling the film into a cylinder. The heat transfer rate was estimated from an energy balance on the water stream using measurements

18

obtained with the same instrumentation described in the previous section. The temperatures at the end of the stack adjacent to each heat exchanger were measured with thermocouples located near the centerline.
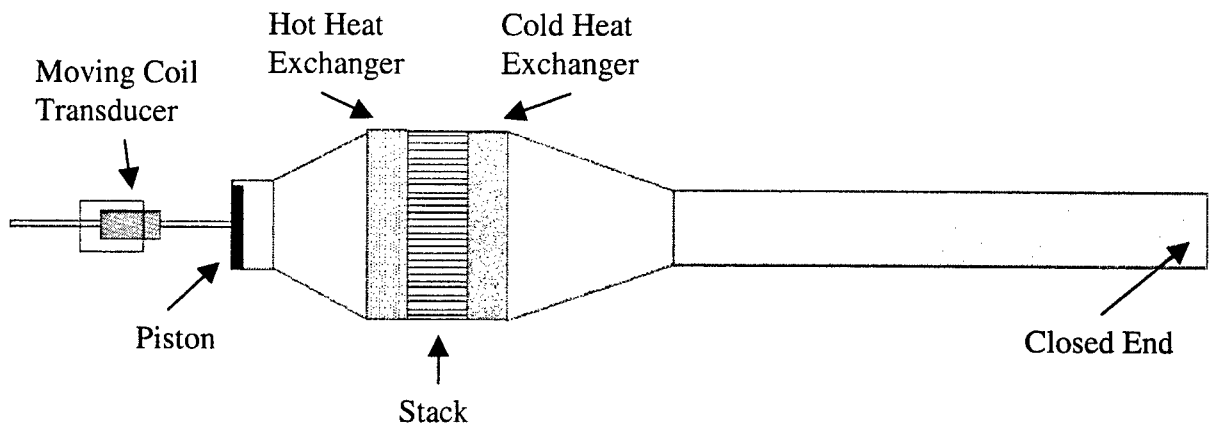
Figure 7: Schematic of Thermoacoustic Cooler.
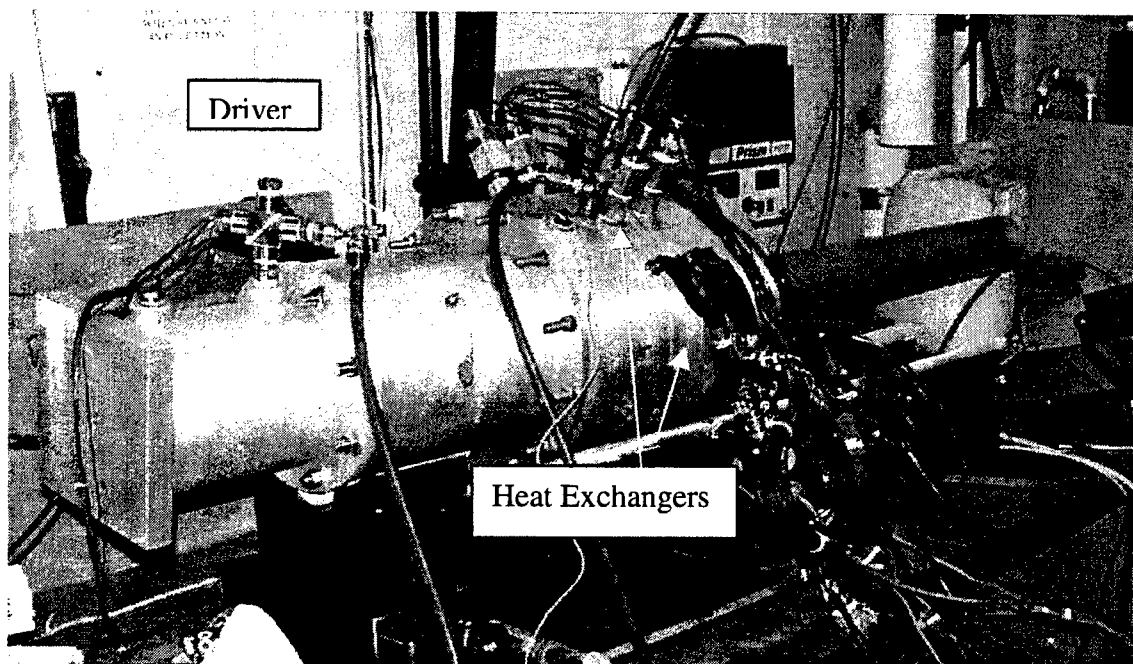
Figure 8: Picture of the Thermoacoustic Cooler.

4.0 Experimental Procedures

4.1 Steady Flow Experimental Procedures

The steady flow tests were designed to conform to the ARI Standard 410 for Forced Circulation Air-Cooling and Air-Heating Coils (www.ari.org). This standard establishes the proper flow conditions of the primary and secondary loops, and outlines procedures for varying the flow conditions.

The data were gathered using a Hewlett Packard 75000 Series B data acquisition system with inputs from the two thermocouple arrays, the differential temperature transducer, the water flow meter, and eight thermocouples distributed over the heat exchanger. Hewlett Packard's visual design environment HPVEE was used to control the data acquisition. Each data point was marked with a time reference and was stored in a text file associated with a particular data set. The data was then post-processed using an Excel spreadsheet.

4.2 Oscillating Flow Experimental Procedures

Data acquisition procedures in the thermoacoustic environment were similar to those followed in the steady flow environment. The heat transfer rate was calculated from an energy balance and water side temperature data. It was necessary to use measured dynamic pressure and piston velocity data to determine the particle velocity in the heat exchangers as discussed later.

5.0 Estimation of Heat Transfer Coefficients

For heat transfer in steady flow, a local heat transfer coefficient is defined as the ratio of the heat transfer per unit area to the temperature difference between the surface and "bulk" fluid adjacent to the surface. However, in practice, a global heat transfer coefficient is utilized that is derived from a lumped analysis of the heat exchanger (UA-LMTD or effectiveness-NTU methods). Generally, a global heat transfer coefficient is estimated from an overall heat exchanger conductance (UA) determined from measurements, using existing correlations for secondary fluid heat transfer coefficient and overall fin efficiency. The UA of the heat exchanger is estimated from the measurements as the ratio of heat transfer rate to a log-mean temperature difference between the primary and secondary fluids. The overall heat transfer rate is estimated from primary or secondary fluid temperature differences and flow rate measurements. The heat transfer coefficient data are often non-dimensionalized using the j-Colburn factor. This non-dimensional presentation allows extrapolation to different gases and operating conditions. The j-Colburn factor data are usually correlated in terms of the Reynolds number.

For the purpose of modeling heat exchangers within a thermoacoustic device, it is more convenient to define a local heat transfer coefficient as the ratio of the heat transfer per unit surface area to the temperature difference between the heat exchanger surface and the time-average thermoacoustic fluid temperature at the end of the stack adjacent to the heat exchanger. Previous researchers have estimated heat transfer coefficients for thermoacoustic heat exchangers by assuming conduction across a laminar boundary layer (Minner, 1996). However, results from these calculations have never been compared with measured values.

In the current study, global thermoacoustic fluid heat transfer coefficients were estimated from overall heat exchanger conductances (UA) determined from measurements, using existing correlations for secondary fluid heat transfer coefficient and overall fin efficiency. This global heat transfer coefficient is consistent with a lumped analysis of the heat exchanger that includes the effects of temperature variations within the fins and secondary fluid. The UA of the heat exchanger was estimated from the measurements as the ratio of heat transfer rate to a log-mean temperature difference between the secondary fluid and the time-averaged thermoacoustic fluid temperature near the stack. The overall heat transfer rate was estimated from secondary fluid temperature and flow rate measurements. The heat transfer coefficient data were non-dimensionalized using the j-Colburn factor. In this case, the j-Colburn factor data were correlated in terms of an acoustic Reynolds, defined using a root-mean-square (rms) velocity within the heat exchanger. The rms velocities at the heat exchangers were estimated from linear-acoustic theory using dynamic pressure and velocity measurements at the driver face of the thermoacoustic device and DELTAE (Ward, 1993).

The following subsections provide details of the calculations used to estimate heat transfer coefficients from both physical descriptions and measured performance data.

5.1 Steady Flow Calculations

5.1.1 Theoretical Calculations

Many general correlations exist for estimating global heat transfer coefficients for steady flow over fin-tube geometries given physical dimensions and properties. For heat exchangers with smooth fins, a correlation developed by Gray and Webb [1986] expresses heat transfer data in terms of a j-Colburn factor according to the following correlation.

$$j = \frac{Nu}{Re\,Pr^{1/3}} = \left(.991 \times \left(2.24\,Re^{-.092}\left(\frac{1}{4}\right)^{-.031}\right)^{1.821}\right)\left(.14\,Re^{-.328}\left(\frac{S_t}{S_l}\right)^{-.502}\left(\frac{s}{D_o}\right)^{.0312}\right) \quad (1)$$

where the tube spacing normal to the flow is given by S_t, the tube spacing in the air flow direction is given by S_l (This factor was ignored in this study because there is one row in the heat exchanger), the spacing between adjacent fins is s, D_o represents the tube diameter for the secondary flow, and Nu, Re, and Pr refer to standard dimensionless groups defined in the nomenclature.

5.1.2 Calculations from Data

The overall conductance of a heat exchanger operating in steady flow and at steady state can be estimated from experimental data using a log-mean temperature difference model. A cross-flow heat exchanger is considered in this study with water flowing through the tubes and air flowing over the finned tubes. For the operating conditions considered in this study, the capacitance rate (product of mass flow rate and specific heat) of the water is much greater than that of the air. In this case, the overall heat exchanger conductance is estimated according to

$$UA = \frac{\dot{Q}}{LMTD} \quad (2)$$

where $\dot{Q}$ is the heat transfer rate determined from measurements and $LMTD$ is the log-mean temperature difference defined as

$$LMTD_s = \frac{(T_{h,i} - T_{c,o}) - (T_{h,o} - T_{c,i})}{\ln\left\{\frac{T_{h,i} - T_{c,o}}{T_{h,o} - T_{c,i}}\right\}} \quad (3)$$

and where s denotes steady flow and T_{hi}, T_{ci}, T_{ho}, and T_{co} are the inlet (i) and outlet (o) temperatures of the hot (h) and cold (c) streams.

The heat transfer rate is determined from measurements using an energy balance on the hot or cold stream as

$$\dot{Q} = \dot{m}_h c_{ph}(T_{h,i} - T_{h,o})$$ (4)

or

$$\dot{Q} = \dot{m}_c c_{pc}(T_{c,o} - T_{c,i})$$ (5)

where $\dot{m}$ is mass flow rate, C_p is constant pressure specific heat, and the subscripts h and c denote hot or cold stream conditions, respectively.

The heat exchanger conductance can be estimated from measurements using equations 2, 3, and 4 (or 5). The heat transfer conductance can then be related to the hot and cold stream heat transfer characteristics according to

$$UA = \frac{1}{\dfrac{1}{\eta_o h_o A_o} + R_{tw} + \dfrac{1}{h_i A_i}}$$ (6)

where η, h, and A are overall fin efficiency, global heat transfer coefficient, and surface area, R_{tw} is the resistance of the tube wall, and the subscripts o and i denote outer and inner surfaces of the fin-tube heat exchanger.

Generally, the outer global heat transfer coefficient (h_o) is estimated from data by solving equation 6 using a UA determined from measurements, known surface areas, and theoretical estimates for R_{tw}, h_i, and η_o.

24

The inside heat transfer coefficient, h_i, for the fin tube heat exchangers can be conveniently found for a range of Reynolds number ($3000 < Re_D < 5 \times 10^6$) using the Gnielinski correlation (Incropera and Dewitt, 1996)

$$\overline{Nu}_D = \frac{(f_G/8)(Re_D - 1000)Pr}{1 + 12.7(f_G/8)^{1/2}(Pr^{2/3} - 1)} \qquad (7)$$

where $\overline{Nu}_D$ is the Nusselt number and is related to the heat transfer coefficient according to

$$\overline{Nu}_D = \frac{h_i D}{k} \qquad (8)$$

where h_i is the inside convection heat transfer coefficient, k is the thermal conductivity and D is the inner diameter of the finned tube. Therefore h_i can be calculated from Egs. 7 and 8.

Also, the friction factor, f_G, can be found by

$$f_G = (.79 \ln Re_D - 1.64)^{-2} \qquad (9)$$

and the Reynolds number based up tube diameter is given by

$$Re_D = \frac{uD\rho}{\mu} \qquad (10)$$

where u is the fluid velocity, D is the inner diameter of the finned tube, ρ is the fluid density, and μ is the dynamic viscosity. Due to the different tube geometry of the microchannel design, Modine Manufacturing Corporation recommends using the Sieder-Tate correlation,

$$\overline{Nu}_D = 1.86 \left(\frac{Re_D Pr}{L/D_h} \right)^{1/3} \left(\frac{\mu}{\mu_s} \right)^{.14} \qquad (11)$$

where L is the tube length, μ is the dynamic fluid viscosity, μ_s is dynamic viscosity of the fluid at the tube surface, and Pr is the Prandtl number and D_h is the hydraulic diameter of the non circular tube which is defined as

$$D_h \equiv \frac{4A_{cs}}{P} \qquad (12)$$

where A_{cs} is the cross-sectional area and P is the wetted perimeter of the finned tube.

The tube wall resistance and external fin efficiency are basic quantities found in most heat transfer textbooks (Incropera and Dewitt, 1996) and are defined by:

$$R_{tw} = \frac{\ln(D_o/D_i)}{2\pi L_t\, k_t} \qquad (13)$$

and

$$\eta_o = 1 - \frac{A_f}{A}(1 - \eta_f) \qquad (14)$$

where

$$\eta_f = \frac{\tanh(mL)}{mL} \qquad (15)$$

and

$$m = \frac{Ph_o}{kA_{fc}} \qquad (16)$$

In equations 13-16, D_o and D_i are the external and internal diameters, L_t is the total tube length, k_t is the thermal conductivity of the tube, A_f is the total fin surface area, A is the total heat exchanger surface area, L is the length of a single fin, P is the fin perimeter, h_o is the external heat transfer coefficient, k is the thermal conductivity of the fin material, and A_{fc} is the fin cross-sectional area.

In order to non-dimensionalize the data for various gases and to facilitate comparison with theoretical calculations, the experimental outer heat transfer coefficient are converted into the j-Colburn factor define as:

26

$$j = St \, \mathrm{Pr}^{2/3} = \frac{\overline{Nu}_D}{\mathrm{Re}_D \, \mathrm{Pr}^{1/3}} \, . \tag{17}$$

where $\overline{Nu}_D$ and Re_D are Nusselt number and Reynolds number, respectively, for the air side

flow. The hydraulic diameter, D_h, in this case is conveniently calculated by

$$D_h = \frac{4LA_c}{A} \tag{18}$$

where L is the fin length (length of flow path), A_c is the flow area and A is the total heat

exchanger surface area.(Gray and Webb, 1986). The detailed calculation for D_h is given in

appendix IX

5.2 Description of Oscillating Flow Calculations

5.2.1 Theoretical Calculations

A general definition for local heat transfer coefficient for a surface in contact with a fluid

in internal flow is:

$$h = \frac{-k \, \partial T/\partial y \big|_{y=0}}{T_s - T_m} \tag{19}$$

where k is the thermal conductivity of the fluid, T_s is the surface temperature and T_m is the mean

temperature of the fluid over the surface of the heat exchanger. In order to provide a theoretical

method for calculating heat transfer coefficients in an oscillating flow, several investigators have

proposed the use of equation 19 with the mean fluid temperature taken to be the time-averaged

fluid temperature at the stack end adjacent to the heat exchanger, $\partial T/\partial y \big|_{y=0}$ approximated by

the temperature difference between the surface and the time-averaged stack end fluid

temperature divided by the thermal boundary layer thickness, Δy_k (Minner, 1996). The

27

boundary layer thickness is assumed to be the minimum of the half plate spacing of the heat exchanger (y_0) and the thermal penetration depth (δ_t) where

$$\delta_t = \sqrt{\frac{2\alpha}{\omega}} \qquad\qquad (20)$$

and

$$\alpha = \frac{k}{\rho c_p} . \qquad\qquad (21)$$

With these approximations, equation 17 reduces to

$$h = \frac{k}{\min(y_o, \delta_t)} . \qquad\qquad (22)$$

For an ideal thermoacoustic heat exchanger, only the surface area within one particle displacement of the stack can participate in the heat transfer. Therefore, a global heat transfer coefficient that accounts for the "dead" surface area of the heat exchanger is estimated as

$$h = \frac{k}{\min(y_o, \delta_t)} \cdot \frac{x_p}{x_{hx}} \qquad\qquad (23)$$

where x_p is the distance associated with a particle displacement at the heat exchanger and x_{hx} is the width of the heat exchanger in the direction of thermoacoustic flow (Minner, 1996).

It has also been proposed that heat transfer coefficients for oscillating flow conditions could be estimated using steady-flow correlations with the Reynolds number evaluated using the acoustic velocity (rms of the oscillating velocity) (Mozurkewich (1995). Both the boundary layer approximation and use of steady-flow correlations are investigated as approaches for predicting heat transfer coefficients in oscillating flow.

5.2.2 Calculations from Data

For cases where the heat exchanger is placed in an acoustically oscillating flow (within a thermoacoustic system), equations 2, 3, 4 (or 5) and 6 are also used to estimate the outer (thermoacoustic fluid to surface) heat transfer coefficient from measurements and the heat transfer coefficient is transformed into the j-Colburn factor using equation 17. However, the inlet and outlet primary fluid temperatures are not defined for the oscillating flow stream and little temperature change can be attributed to fluid particles oscillating either over the heat exchanger or between the heat exchanger and the stack. In this case, the log mean temperature difference was calculated by

$$LMTD_{tac} = \frac{(T_{w,o} - T_{w,i})}{Ln\left\{\dfrac{T_s - T_{w,i}}{T_s - T_{w,o}}\right\}} \tag{24}$$

where tac stands for thermoacoustic, $T_{w,o}$ and $T_{w,i}$ are the water outlet and inlet temperatures, and T_s is the stack end temperature. Finally, the steady-state energy balance for the water stream is used to determine the heat transfer rate from measurements.

In this study, root mean square (rms) acoustic particle velocity was used to correlate j-Colburn factors for oscillating flow conditions. Unfortunately, it was not possible to measure the acoustic particle velocity in the heat exchangers directly. This problem was solved by using a thermoacoustic modeling software developed at Los Alamos National Laboratory, DeltaE (Ward 1993), to compute the local root-mean square velocity. This estimate of the particle velocity was then used in computing an acoustic Reynolds number. The acoustic Reynolds number was used in correlating the j-Colburn factors.

6.0 Results

6.1 Steady Flow Results

The data for the steady flow results are presented in two forms. Figure 9 is a graph of the j-Colburn factor versus the Reynolds number. Figure 10 shows the heat transfer coefficient versus the Reynolds number. In each case, the heat transfer coefficients were calculated using heat transfer results determined from air-side and water-side measurements. For each airflow rate, several different water flowrates were used in order to verify consistency. The differences between the air-side and water-side results are an indication of experimental errors. Generally, the air-side and water-side results are within about 20%.

The heat transfer coefficient increases with Reynolds number, as expected. The fin-tube heat exchanger results were compared with the Gray-Webb correlation, shown as a solid line in figure 9. The test results compare very well with the correlation. No similar correlation could be found in the literature for the micro-channel heat exchanger. The heat transfer coefficients for the microchannel heat exchanger are significantly greater than those of the fin-tube heat exchanger. Note the different hydraulic diameter for the two exchangers.
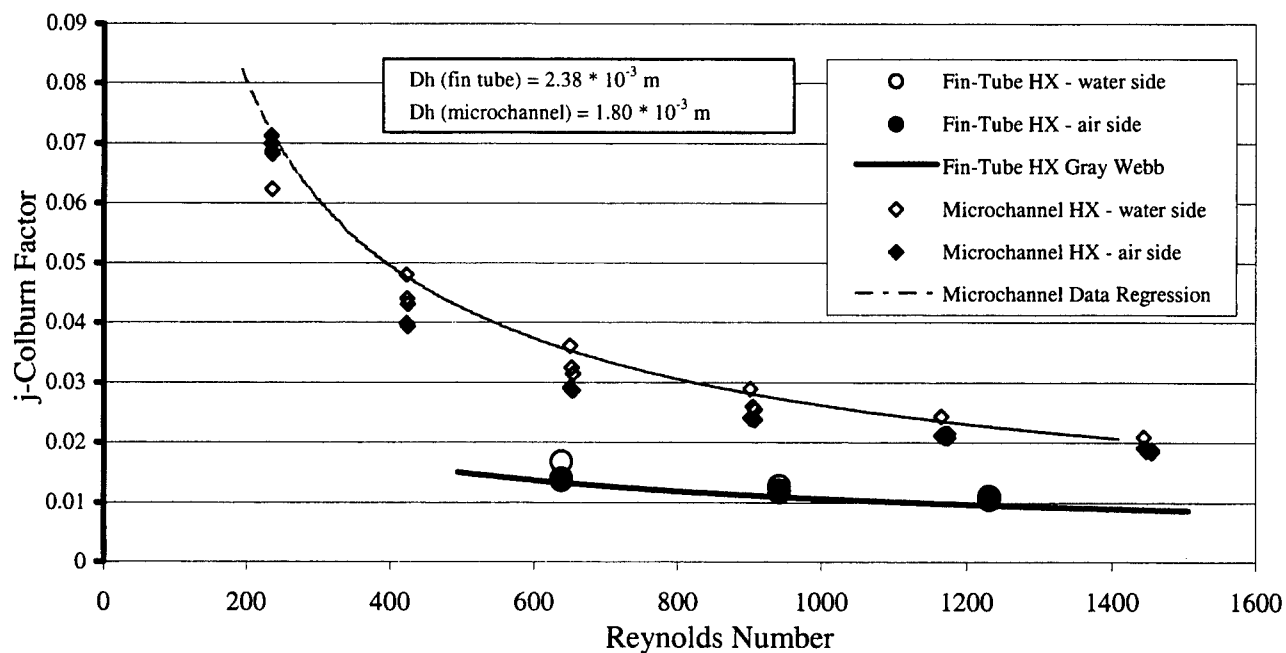
Figure 9. *Steady Flow j-Colburn vs. Reynolds Number*
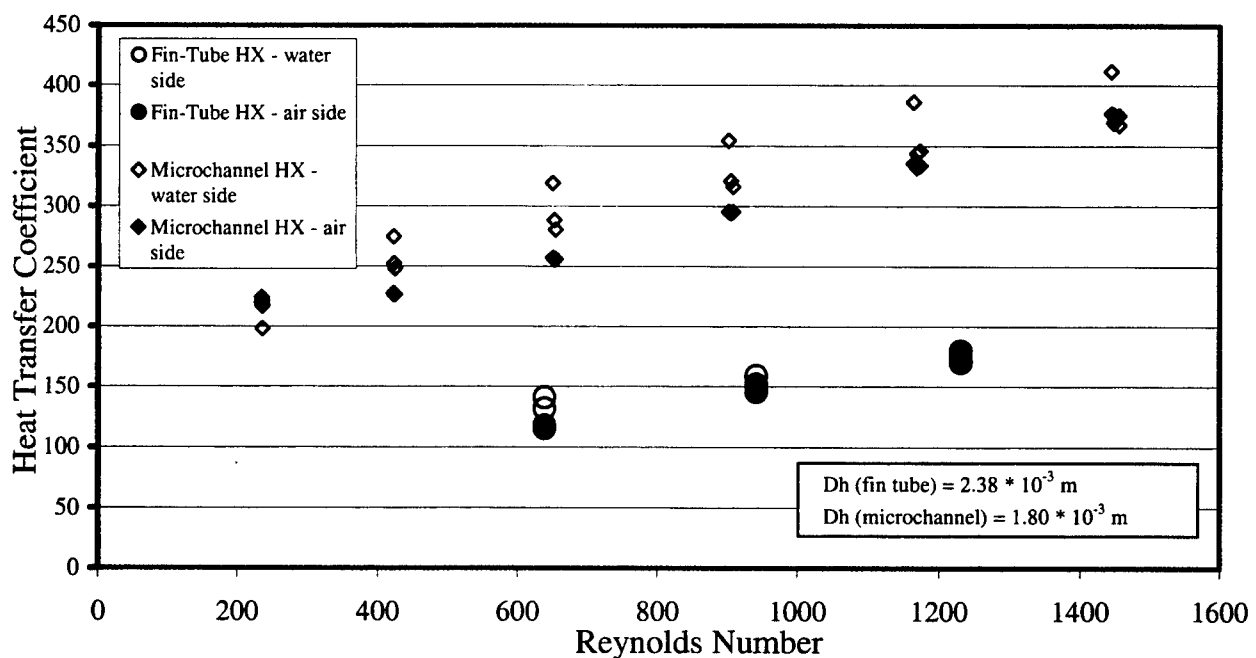
Figure 10. *Steady Flow Heat Transfer Coefficient* $(W/m^2 \cdot K)$ *vs. Reynolds Number*

31

6.2 Performance of the Heat Exchangers in Oscillating Flow

The results for the fin-tube heat exchanger only are shown in figures 11 and 12, where

the j-factor and the heat transfer coefficient h are plotted versus acoustic Reynolds number,

respectively. Unfortunately, heat gains originating from the driver biased much of the early data

and only a very small subset of the original data was useable. In order to determine which data

were unusable, a first law balance was used. The sum of the measured power input and the

pumped heat were compared to the measured heat rejected on the hot side heat exchanger. Data

points with an energy balance disparity greater than 15% were rejected. As can be seen from the

fin-tube results, only a limited number of data points passed the test. This caused poor resolution

in the data. Nevertheless, the data clearly shows a marked increase in performance for the

microchannel heat exchanger. Also, it is obvious that the boundary layer approximation

provides estimates for heat transfer coefficients that are extremely conservative.
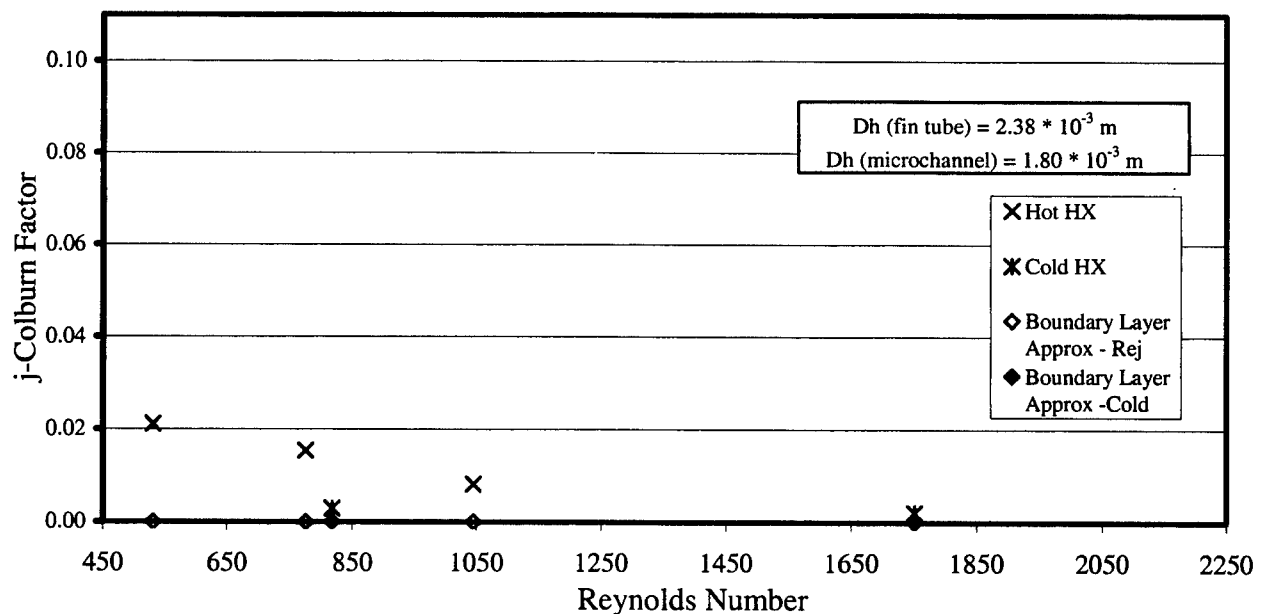
Figure 11. *j-Colburn vs. Reynolds Number for Periodic Flow; Fin-Tube Heat Exchanger.*
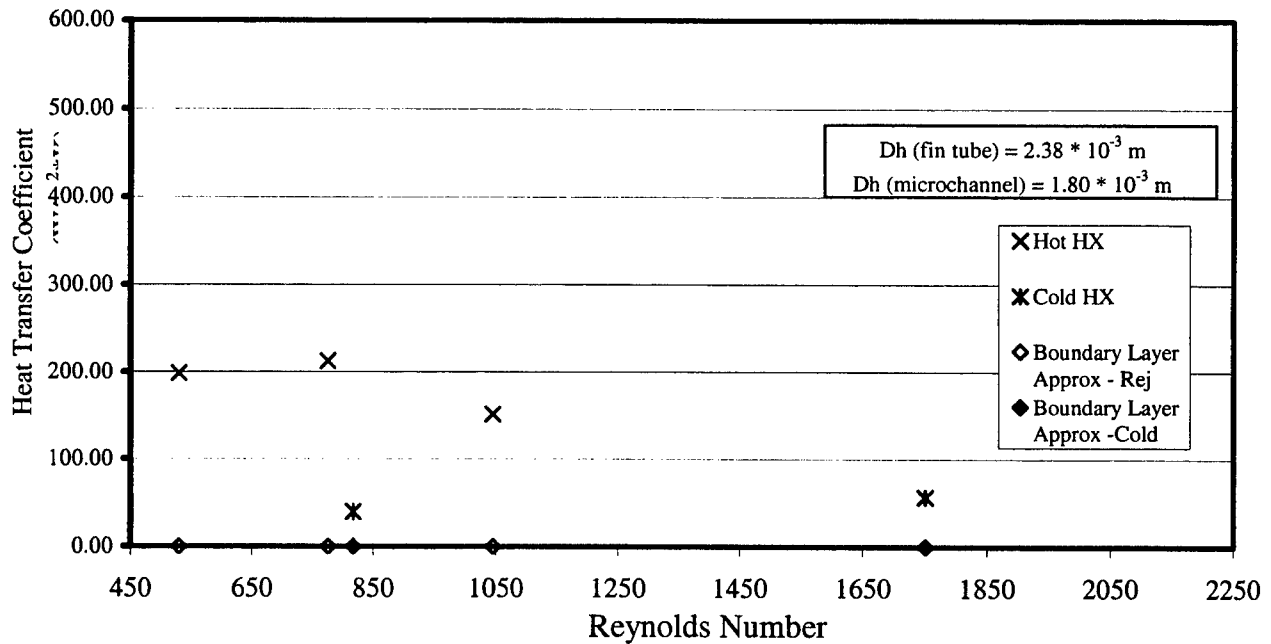
Figure 12. *Heat Transfer Coefficient (W/m²K) vs. Reynolds Number for Periodic Flow; Fin-Tube Heat Exchanger*

Figures 13 and 14 show the results for the micro-channel heat exchangers. In each case, results for both the hot and cold heat exchangers in the thermoacoustic system are presented. In addition to the experimental results, the figures show the boundary layer conduction approximation that is often used in thermoacoustics to predict heat transfer. For the microchannel heat exchanger, several tests were performed where heat leak from the driver was kept relatively small. In order to reduce the effects of heat gains from the driver, the driver was only operated short periods of time for each data point. Using this method, it was possible to reduce, but not completely eliminate, the energy imbalances. As can be seen from figures 13 and 14, the data appears to be consistent, and several interesting trends appear. Firstly, the measured heat exchanger performance at low Reynolds numbers is much greater than that predicted using the boundary layer calculation commonly used in thermoacoustics. As mentioned earlier, these models assume that the heat transfer coefficient is a result of conduction across the thermal

boundary layer. It appears that this approach works well at high Reynolds numbers, but significantly underpredicts the j-Colburn factor at low Reynolds numbers. This could have a significant impact on the prediction and the design optimization of the performance of thermoacoustic systems.

A second observation is that the steady flow regression model seems to provide a reasonably good approximation for the thermoacoustic j-Colburn factor when evaluated with acoustic Reynolds numbers. It is obvious from the figure that the steady flow regression provides a better estimate than the boundary layer approximation. This can be also observed in figure 15which compares the regression models for the thermoacoustic and steady flow data of the microchannel heat exchanger.

Another important trend is a difference in the functional dependence on Reynolds number between the hot and cold heat exchangers. It is believed that this difference is due an inaccurate characterization of the stack-end temperatures. In order to investigate this further, a radial array of thermocouples was installed at the stack ends. This array revealed that there is an obvious dependence of stack temperature upon radial position. It has been postulated that this is due to the influence of the container's aluminum walls and it obviously implies that using one temperature probe to calculate the log-mean temperature difference is misleading since it does not properly take into account the temperature distribution. Using data from the thermocouple array, a spatially averaged temperature distribution was calculated and used to calculate a new j-Colburn factor. The results appear in figure 16 for a limited number of data points. It can be seen that this new approach yields closer agreement between the hot and cold heat exchanger heat transfer coefficient relationships. However, in this case, the steady-flow correlation tends to over predict the heat transfer coefficients.

Finally, the data show that the microchannel heat exchanger performs significantly better than the fin tube heat exchanger when operating in an oscillating flow environment. These results are shown in Figure 17 and are consistent with the steady-flow results.
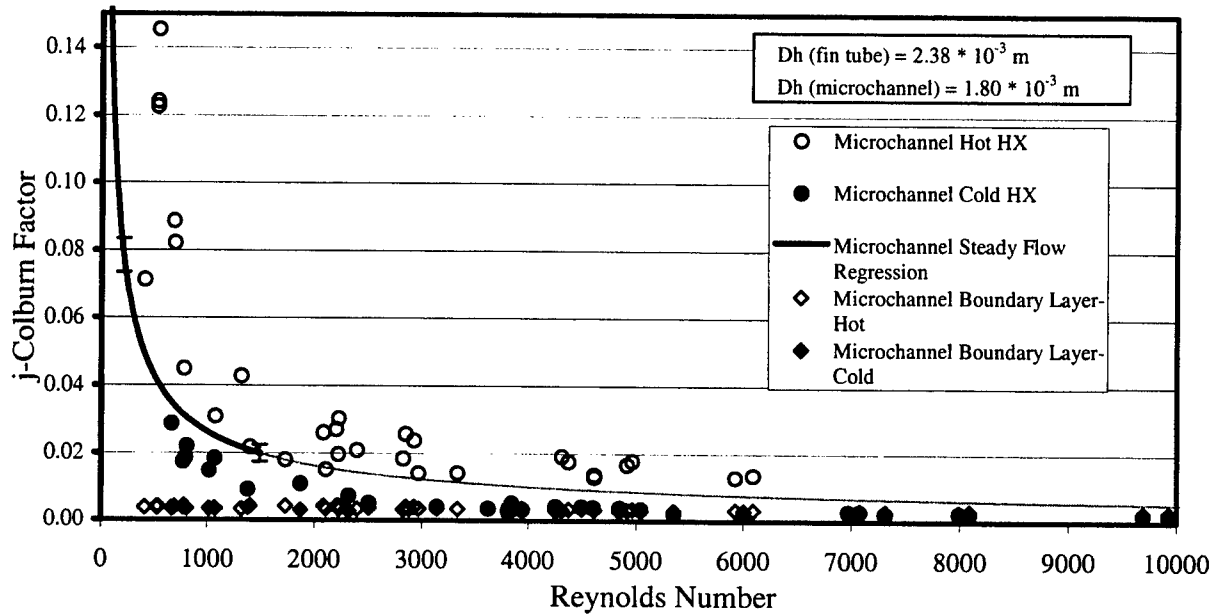
Figure 13. *j-Colburn vs. Reynolds Number for Periodic Flow; Microchannel ; Dotted line denotes the extrapolation of the experimental data*
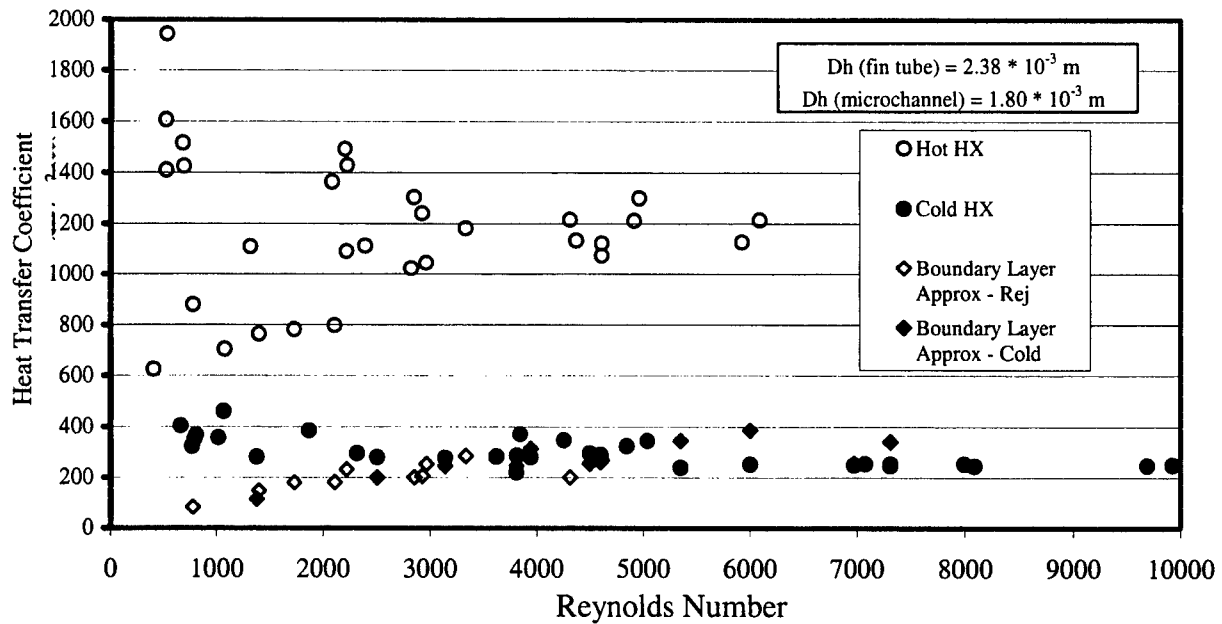
Figure 14. *Heat Transfer Coefficient* ($W/m^2 K$) *vs. Acoustic Reynolds Number for Periodic*
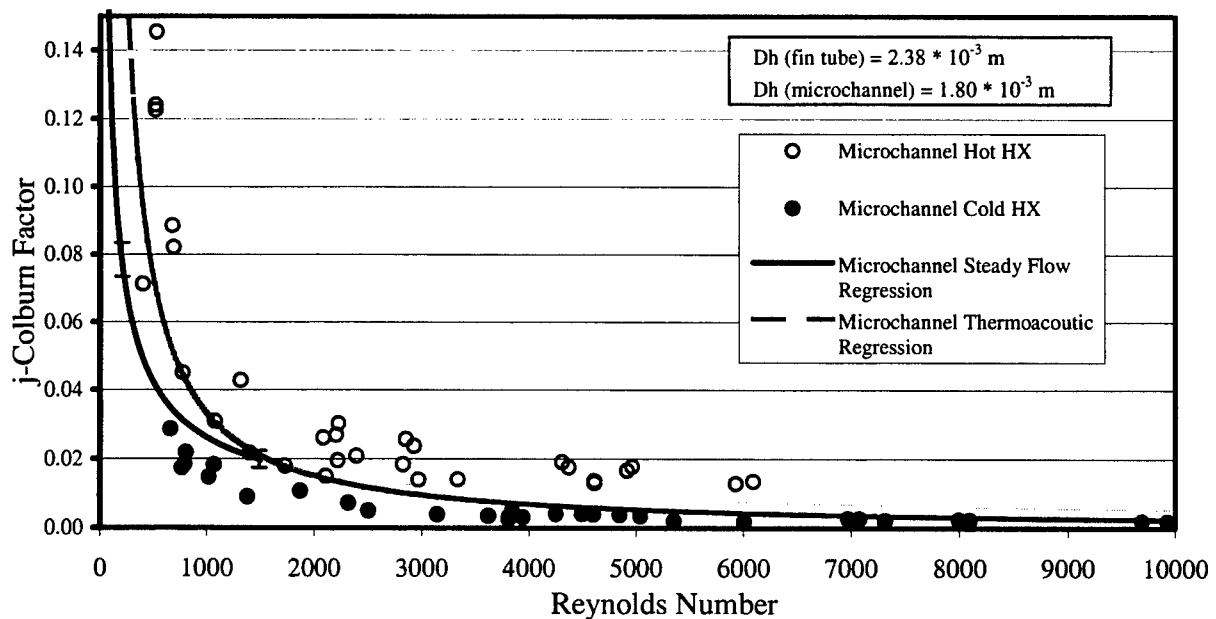
Flow; Microchannel

Figure 15. *j-Colburn vs. Acoustic Reynolds Number Regression; Microchannel Heat Exchanger ;Dotted line denotes the extrapolation of the experimental data*
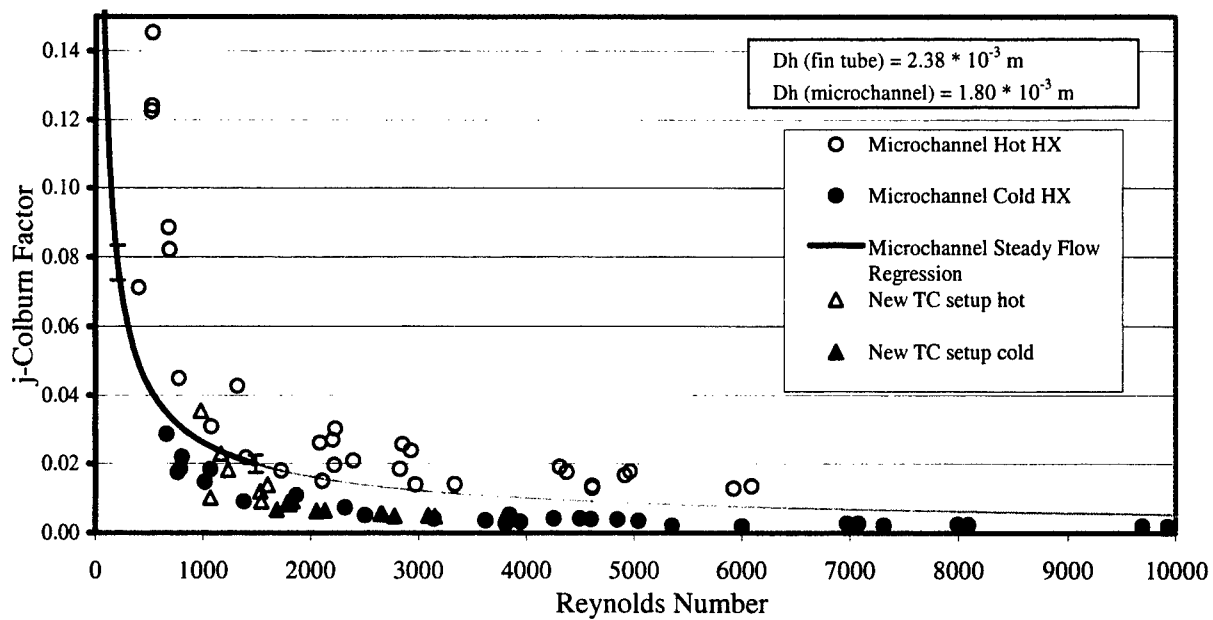
Figure 16. *j-Colburn vs. Acoustic Reynolds Number; Microchannel Heat Exchanger, Computed from Radial Thermocouple Array Data*
;Dotted line denotes the extrapolation of the experimental data
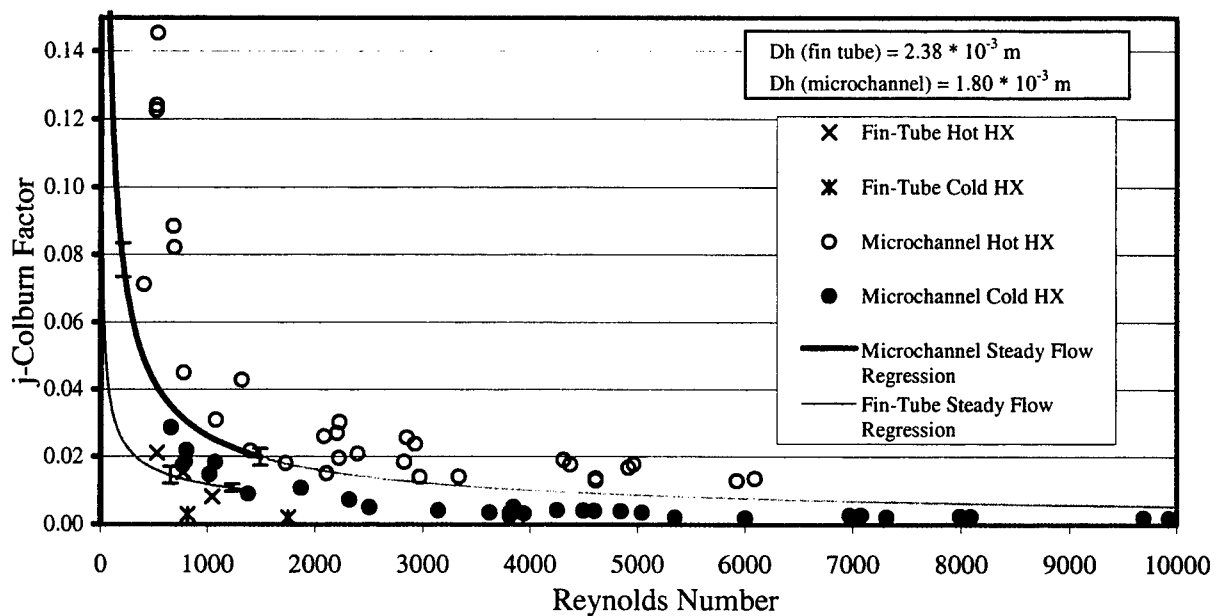
Figure 17. *j-Colburn vs. Acoustic Reynolds Number: Comparison of Heat Exchangers*
;Dotted line denotes the extrapolation of the experimental data

7.0 Conclusions and Future Work

The performance of two different heat exchangers was measured in steady and pulsating flows. The results suggest that the thermoacoustic heat transfer could be predicted using steady flow correlations with acoustic Reynolds numbers. This could simplify the heat transfer calculations and would increase the accuracy of the current models. In order to confirm this, a new battery of tests would need to be designed and implemented. It would be necessary to run the tests on several different heat exchanger types and compare them to the steady flow correlations. It should be noted that there is an uncertainty in the value of the particle velocity because it is being estimated from linear acoustic models (DeltaE calculation). This value could also be affected by possible streaming (i.e. acoustically driven steady flows) effects within the thermoacoustic device. These possible errors could be assessed and corrected by implementing a hot-wire anemometer into the system at specific points to measure the total (AC and DC) velocity.

The accuracy of the test data for the pulsating flow cases is strongly dependent on the magnitude of the heat flux. In its current configuration, the thermoacoustic system does not allow very high heat fluxes to be achieved, the the system is affected by heat production from the driver, and thermal conduction though the shell. Temperatures gradients are small. It is difficult to accurately measure small temperatures, especially when considering that the thermoacoustic system is closed and pressurized. The best solution for eliminating this source of error is to continue to work to increase the heat transfer values and install a driver cooling system.

LIST OF REFERENCES

Brewster, J., Raspet, R., and Bass, H. 1997. "Temperature discontinuities between elements of thermoacoustic devices." *J. Acoust. Soc. Am.*, Vol 102, No 6, pp. 3355-3360.

"Forced Circulation Air-Cooling and Air-Heating Coils," Standard 410. 1991. Air-Conditioning and Refrigeration Institute, Arlington.

Garrett, S., Perkins, D, and Gopinath, A. 1994. "Thermoacousitc refrigerator heat exchangers: Design, analysis, and fabrication." *Proceedings of the 10ᵗʰ International Heat Transfer Conference*. Taylor & Francis, San Francisco, Vol. 4, pp.375-380.

Gray, D.L. and Webb, R.L. 1986. "Heat transfer and friction correlations for plate finned-tube heat exchangers having plain fins." *Proceedings of the 8ᵗʰ International Heat Transfer Conference*. Taylor & Francis, London, San Francisco, pp.2745-2750.

Incropera, F. and Dewitt, D. 1996. <u>Fundamentals of Heat and Mass Transfer</u>. New York. Wiley and Sons.

Minner, B., 1996. "Design optimization for thermoacoustic cooling systems." Master thesis, Engineering Dept., Purdue University.

Minner, B., Mongeau, L., Braun, J., 2000. "Experimental Investigation of a thermoacoustic cooler prototype." *Proceedings of the 4ᵗʰ IIR-Gustav Lorentzen Conference on Natural Working Fluids at Purdue*. Purdue University, West Lafayette, pp 447-456.

Mozurkewich, George. 1995. "Heat transfer form a cylinder in an acoustic standing wave." *J. Acoust. Soc. Am.*, Vol 98, No 4, pp. 2209-2216.

Mozurkewich, George. 1998. "Time-average temperature distribution in a thermoacoustic stack." *J. Acoust. Soc. Am.*, Vol 103, No 1, pp. 380-388.

Mozurkewich, George. 1998. "A model for transverse heat transfer in thermoacoustics." *J. Acoust. Soc. Am.*, Vol 103, No 6, pp. 3318-3326.

Mozurkewich, George. 2000. Personal Correspondence

Rich, D.G. 1976. "The effect of fin spacing on the heat transfer and friction performance of multi-row, smooth plate fin-and-tube heat exchangers." *ASHRAE Transactions*, Vol. 70 pt. 2 pp. 137-145.

Swift, Greg. 1992. "Analysis and performance of a large thermoacoustic engine." *J. Acoust. Soc. Am.*, Vol 92, No 3, pp. 1551-1563.

Swift, Greg. *Thermoacoustics: A unifying perspective for some engines and refrigerators.* Fourth Draft. Condensed Matter and Thermal Physics Group Los Alamos National Laboratory. LA-UR 99-895. Autumn 1999.

Wang, C-C., Lee, C-J,, Chang, C-T., and Lin, S-P. 1998. "Heat transfer and friction correlation for compact louvered fin-and-tube heat exchangers." *International Journal of Heat and Mass Transfer*, Vol. 42, pp. 1945-1956.

Ward, W., and Swift G. 1993. "Design environment for low-amplitude thermoacoustic engines." J. Acoust. Soc. Am. Vol. 95, 3671-3672

Wetzel, M., Herman, C. 1999. "Experimental study of thermoacoustic effects on a single plate Part II: Heat transfer." *Heat and Mass Transfer*, Vol. 35, pp. 433-441.

Wetzel, M., Herman, C. 2000. "Experimental study of thermoacoustic effects on a single plate Part I: Temperature fields." *Heat and Mass Transfer*, Vol. 36, pp. 7-20.

Zhao, Z. and Avediaian, C.T. 1997. "Enhancing forced air convection heat transfer from an array of parallel plate fins using a heat pipe." *International Journal Heat Mass Transfer*, Vol. 40, pp. 3135-3147.

APPENDICES

Appendix I: Table of Thermoacoustic Raw Data for the Microchannel Heat Exchangers

Measurement	units	Data Point											
		1	2	3	4	5	6	7	8	9	10	11	12
pressure	psi	200	200	200	200	300	300	300	300	300	200	200	300
mix		0.55	0.55	0.55	0.55	0.55	0.55	0.55	0.3447	0.3447	0.3447	0.3447	0.216
freq	Hz	172.10	172.10	172.10	172.08	173.25	173.25	173.25	143.90	144.10	144.00	144.25	133.70
Wac	W	89.22	65.77	36.87	118.46	62.02	104.24	125.94	83.71	119.14	76.16	114.44	62.91
Qc	W	109.69	91.17	62.00	126.69	64.02	88.66	99.49	84.94	102.55	104.56	127.23	63.30
Qh	W	175.15	144.91	95.14	230.28	131.31	195.36	224.53	179.59	227.00	186.10	244.12	139.41
DTh	degC	0.88	0.73	0.48	1.15	0.66	0.98	1.12	0.90	1.14	0.94	1.23	0.70
DTc	degC	0.67	0.56	0.38	0.77	0.39	0.54	0.61	0.50	0.60	0.58	0.70	0.35
Vrateh	L/sec	0.05	0.05	0.05	0.05	0.05	0.05	0.05	0.05	0.05	0.05	0.05	0.05
Vratec	L/sec	0.04	0.04	0.04	0.04	0.04	0.04	0.04	0.04	0.04	0.04	0.04	0.04
stack DT	degC	6.33	5.28	3.49	7.47	4.58	6.16	6.80	5.71	6.95	5.90	7.53	4.31
p0	kPa	67065	53704.05	31417.2	82159	80369	111302	124162	118582.5	142679.5	73644	94564.5	105569
Qc+Wac-Qh	balance	23.76	12.03	3.73	14.86	-5.27	-2.46	0.89	-10.94	-5.32	-5.38	-2.44	-13.20
Thi	degC	22.91	22.91	22.93	22.97	22.98	22.96	22.97	22.88	22.88	23.01	23.00	22.92
Tci	degC	22.81	22.81	22.81	22.85	22.86	22.84	22.83	22.75	22.76	22.90	22.89	22.80
wtr-stk	DT -h deg C	-3.49	-2.91	-1.84	-4.21	-2.60	-3.61	-4.03	-3.30	-4.12	-3.29	-4.35	-2.50
wtr-stk	DT -c deg C	2.74	2.26	1.54	3.14	1.86	2.43	2.64	2.28	2.71	2.50	3.08	1.69
piston vel	(m/s)	1.31	0.96	0.72	1.23	0.84	1.07	1.15	0.97	1.11	0.90	1.06	0.65
pdr phase		126.10	125.03	124.16	128.73	119.21	120.79	122.06	-119.03	-121.70	-130.61	-134.58	-125.57
Tavgh	degC	23.35	23.28	23.17	23.55	23.31	23.45	23.53	23.33	23.45	23.48	23.62	23.27
Tavgc	degC	23.14	23.09	23.00	23.23	23.05	23.11	23.14	23.00	23.06	23.19	23.25	22.98
Mtbh	degC	26.39	25.73	24.64	27.21	25.39	26.42	26.94	26.10	26.83	26.13	27.10	25.35
Mtbc	degC	19.24	19.77	20.44	18.91	20.27	19.65	19.52	19.96	19.62	19.86	19.39	20.65
Inbal/(Qc+Wac)*100		11.95	7.67	3.77	6.06	4.18	1.28	0.40	6.49	2.40	2.97	1.01	10.45
GBFDC-h	degC	26.82	26.16	25.04	27.74	25.77	26.70	27.20	26.63	27.42	26.77	27.82	25.77
GBFSQ-c	degC	20.16	20.57	21.28	19.84	21.06	20.43	20.19	20.69	20.40	20.54	20.05	21.31
GDQ38-c	degC	18.98	19.57	20.49	18.51	20.22	19.43	19.15	19.81	19.34	19.56	18.98	20.58
Mfn-h	degC	26.89	26.12	25.08	27.66	25.81	26.85	27.33	26.53	27.25	26.52	27.58	25.77
Mfn-c	degC	19.74	20.16	20.87	19.36	20.68	20.08	19.90	20.38	20.05	20.25	19.86	21.07
GDQ38-h	degC	27.55	26.39	24.86	28.53	25.97	27.28	28.09	27.04	28.19	27.47	28.98	26.29
GDC38-c	degC	19.93	20.34	20.81	19.61	20.93	20.50	20.39	20.64	20.22	20.31	19.79	21.25
GBFSC-h	degC	26.40	25.82	24.77	27.17	25.58	26.57	27.00	26.18	27.00	26.30	27.35	25.42
GBFSC-c	degC	20.07	20.54	21.28	19.71	21.00	20.41	20.20	20.48	20.05	20.40	19.82	21.12
Who	degC	23.88	23.69	23.40	24.21	23.65	23.97	24.14	23.85	24.10	24.00	24.30	23.68
Wco	degC	22.12	22.25	22.46	22.04	22.46	22.25	22.20	22.25	22.18	22.33	22.17	22.51
GBFDC-c	degC	20.01	20.51	21.30	19.71	21.13	20.46	20.22	20.61	20.33	20.52	19.98	21.22
GBFSQ-h	degC	22.50	22.85	23.02	24.01	24.15	24.28	24.49	23.95	24.52	24.31	24.85	24.74
Whi	degC	22.91	22.91	22.93	22.97	22.98	22.96	22.97	22.88	22.88	23.01	23.00	22.92
Wci	degC	22.81	22.81	22.81	22.85	22.86	22.84	22.83	22.75	22.76	22.90	22.89	22.80

Measurement	units	Data Point											
		13	14	15	16	17	18	19	20	21	22	23	24
pressure	psi	300	300	300	250	250	200	200	292	292	250	250	313
mix		0.216	0.216	0.216	0.216	0.216	0.55	0.55	0.466	0.466	0.55	0.55	0.481
freq	Hz	133.75	133.85	133.80	133.70	133.90	168.50	168.50	162.00	160.50	170.25	170.25	162.30
Wac	W	80.99	116.82	120.97	88.47	115.19	103.50	110.43	21.58	63.17	41.30	26.38	55.51
Qc	W	75.24	87.31	92.39	85.32	96.31	109.95	116.78	39.43	86.67	61.72	43.18	82.51
Qh	W	167.07	200.24	220.40	186.78	223.36	228.80	246.52	49.71	131.00	112.28	78.88	122.99
DTh	degC	0.84	1.01	1.11	0.94	1.13	1.16	1.25	0.24	0.63	0.54	0.38	0.56
DTc	degC	0.42	0.48	0.51	0.47	0.53	0.60	0.64	0.26	0.56	0.40	0.28	0.51
Vrateh	L/sec	0.05	0.05	0.05	0.05	0.05	0.05	0.05	0.05	0.05	0.05	0.05	0.05
Vratec	L/sec	0.04	0.04	0.04	0.04	0.04	0.04	0.04	0.04	0.04	0.04	0.04	0.04
stack DT	degC	5.10	6.10	6.52	5.74	6.64	6.83	7.20	1.94	4.18	3.26	2.39	4.09
p0	kPa	121013.5	146558.5	149688	107562.5	123209	75842	79362.5	22155.4	22424.7	19393.95	18770.1	84432.5
Qc+Wac-Qh	balance	-10.84	3.89	-7.04	-12.99	-11.85	-15.36	-19.30	11.30	18.84	-9.26	-9.32	15.03
Thi	degC	22.94	22.94	22.94	23.01	23.02	23.01	23.00	22.55	22.61	22.61	22.61	22.60
Tci	degC	22.82	22.82	22.83	22.90	22.91	22.88	22.89	22.45	22.51	22.51	22.52	22.50

41

wtr-stk	DT -h deg C	-3.00	-3.65	-3.95	-3.40	-3.94	-4.00	-4.24	-1.05	-2.25	-1.82	-1.32	-2.18
wtr-stk	DT -c deg C	1.98	2.34	2.46	2.24	2.59	2.70	2.85	0.79	1.83	1.34	0.98	1.80
piston vel	(m/s)	0.72	0.85	0.90	0.77	0.83	0.97	0.96	0.64	0.60	0.43	0.34	0.65
pdr phase		-127.82	-130.65	-128.11	-132.54	-137.01	138.20	141.01	110.73	132.19	153.77	153.59	126.24
Tavgh	degC	23.37	23.44	23.50	23.48	23.58	23.59	23.62	22.67	22.93	22.88	22.80	22.88
Tavgc	degC	23.03	23.06	23.09	23.13	23.18	23.18	23.21	22.58	22.79	22.71	22.66	22.75
Mtbh	degC	25.86	26.45	26.75	26.26	26.82	26.98	27.21	23.50	24.88	24.33	23.77	24.73
Mtbc	degC	20.45	20.10	20.07	20.26	20.01	19.74	19.49					
Inbal/(Qc+Wac)*100		6.94	1.91	3.30	7.48	5.60	7.19	8.50	18.53	12.58	8.99	13.40	10.89
GBFDC-h	degC	26.35	27.06	27.37	26.90	27.51	27.48	27.72	23.75	25.04	24.60	24.10	24.91
GBFSQ-c	degC	21.10	20.84	20.80	20.99	20.81	20.34	20.27	21.64	20.48	20.91	21.47	20.55
GDQ38-c	degC	20.27	19.89	19.77	20.07	19.72	19.17	18.94	21.33	20.56	20.94	21.49	20.59
Mfn-h	degC	26.31	26.96	27.27	26.78	27.38	27.39	27.67					
Mfn-c	degC	20.90	20.62	20.58	20.78	20.56	20.14	19.95	21.49	20.81	21.20	21.52	20.97
GDQ38-h	degC	27.07	27.80	28.20	27.65	28.50	28.52	28.83	23.36	25.17	24.66	24.06	24.99
GDC38-c	degC	21.03	20.76	20.68	20.85	20.66	20.42	20.16	20.89	19.95	20.42	20.73	20.00
GBFSC-h	degC	25.94	26.58	26.89	26.40	26.96	27.01	27.24	23.60	24.86	24.43	23.93	24.78
GBFSC-c	degC	20.84	20.48	20.37	20.66	20.32	20.18	20.04	21.66	20.67	21.17	21.54	20.69
Who	degC	23.86	24.04	24.15	24.04	24.24	24.25	24.33	22.89	23.40	23.26	23.09	23.28
Wco	degC	22.48	22.40	22.37	22.49	22.42	22.29	22.27	22.33	22.06	22.21	22.36	22.03
GBFDC-c	degC	20.98	20.73	20.64	20.85	20.59	20.28	20.16	21.42	20.92	21.27	21.64	20.96
GBFSQ-h	degC	25.03	25.39	26.03	25.87	26.35	24.93	25.73	23.70	24.98	24.57	24.04	24.79
Whi	degC	22.94	22.94	22.94	23.01	23.02	23.01	23.00	22.55	22.61	22.61	22.61	22.60
Wci	degC	22.82	22.82	22.83	22.90	22.91	22.88	22.89	22.45	22.51	22.51	22.52	22.50

Measurement	units	Data Point						
		25	26	27	28	29	30	31
pressure	psi	313	317	317	300	250	340	340
mix		0.481	0.45	0.45	0.55	0.55	0.404	0.404
freq	Hz	162.30	160.40	159.70	170.60	170.60	149.40	150.90
Wac	W	66.48	22.47	45.42	21.03	21.30	49.62	23.03
Qc	W	92.71	40.95	70.13	38.16	47.38	67.30	33.71
Qh	W	178.44	52.34	106.17	67.52	63.57	104.73	60.69
DTh	degC	0.82	0.24	0.49	0.31	0.29	0.48	0.28
DTc	degC	0.58	0.26	0.44	0.24	0.29	0.41	0.21
Vrateh	L/sec	0.05	0.05	0.05	0.05	0.05	0.05	0.05
Vratec	L/sec	0.04	0.04	0.04	0.04	0.04	0.04	0.04
stack DT	degC	4.72	1.98	3.36	2.04	2.06	3.52	1.97
p0	kPa	98037.5	40063.05	72928	23725.05	23989.65	90194	48496.2
Qc+Wac-Qh	balance	-19.26	11.08	9.38	-8.32	5.11	12.19	-3.94
Thi	degC	22.54	22.72	22.77	22.78	22.93	22.76	22.72
Tci	degC	22.44	22.63	22.67	22.68	22.83	22.65	22.63
wtr-stk	DT -h deg C	-2.58	-1.05	-1.78	-1.12	-1.07	-1.89	-1.08
wtr-stk	DT -c deg C	2.03	0.84	1.48	0.82	0.89	1.53	0.81
piston vel	(m/s)	0.61	0.46	0.42	0.28	0.29	0.36	0.45
pdr phase		134.49	118.73	140.03	159.21	156.77	152.44	116.95
Tavgh	degC	22.95	22.84	23.02	22.93	23.08	23.00	22.86
Tavgc	degC	22.72	22.75	22.89	22.80	22.98	22.86	22.73
Mtbh	degC	25.19	23.81	24.61	23.90	24.01	24.69	23.73
Mtbc	degC							
Inbal/(Qc+Wac)*100		12.10	17.47	8.12	14.06	7.44	10.43	6.95
GBFDC-h	degC	25.42	24.10	24.88	24.23	24.36	24.99	24.04
GBFSQ-c	degC	20.44	21.93	21.22	21.95	21.98	21.14	21.94
GDQ38-c	degC	20.74	21.60	21.15	21.77	21.59	21.21	21.74
Mfn-h	degC							
Mfn-c	degC	20.99	21.70	21.29	21.86	21.75	21.41	21.85
GDQ38-h	degC	25.71	23.65	24.80	24.02	24.01	24.94	23.91
GDC38-c	degC	19.74	21.15	20.57	21.19	21.20	20.56	21.24
GBFSC-h	degC	25.12	23.77	24.56	23.90	24.00	24.65	23.79
GBFSC-c	degC	20.40	21.78	21.20	21.86	21.94	21.13	21.82
Who	degC	23.47	23.06	23.40	23.20	23.31	23.36	23.10
Wco	degC	21.95	22.53	22.39	22.60	22.70	22.42	22.58

GBFDC-c	degC	20.96	21.58	21.24	21.78	21.65	21.38	21.77
GBFSQ-h	degC	25.25	23.83	24.61	23.98	24.07	24.72	23.92
Whi	degC	22.54	22.72	22.77	22.78	22.93	22.76	22.72
Wci	degC	22.44	22.63	22.67	22.68	22.83	22.65	22.63

Measurement	units	Data Point								
		32	33	34	35	36	37	38	39	40
pressure	psi	200	200	200	200	200	200	200	200	200
mix		0.55	0.55	0.55	0.55	0.55	0.55	0.55	0.55	0.55
freq	Hz	169.70	169.70	169.90	169.70	169.70	169.70	169.70	169.90	169.50
Wac	W	48.19	86.56	92.14	75.41	75.96	86.16	69.63	76.50	70.04
Qc	W	74.81	108.31	108.43	91.72	91.85	101.74	90.23	97.93	92.27
Qh	W	100.99	165.48	165.81	150.55	173.90	197.09	179.38	201.30	194.89
DTh	degC	0.60	0.99	0.99	0.90	0.98	1.11	1.01	1.13	1.10
DTc	degC	0.53	0.76	0.77	0.65	0.66	0.73	0.65	0.71	0.66
Vrateh	L/sec	0.04	0.04	0.04	0.04	0.04	0.04	0.04	0.04	0.04
Vratec	L/sec	0.03	0.03	0.03	0.03	0.03	0.03	0.03	0.03	0.03
stack DT	degC	3.15	5.84	5.93	5.49	5.47	6.09	5.45	6.24	6.19
p0	kPa	39354.8	64265.5	65922	55968.05	55479.2	58128	45165.7	44257.55	36761.65
Qc+Wac-Qh	balance	22.02	29.40	34.76	16.59	-6.09	-9.20	-19.51	-26.88	-32.59
Thi	degC	24.18	24.16	24.11	24.02	24.00	24.03	24.05	24.06	24.22
Tci	degC	23.95	23.93	23.88	23.76	23.77	23.80	23.81	23.84	23.98
wtr-stk	DT -h deg C	-3.17	-4.38	-4.51	-4.20	-4.27	-4.50	-4.08	-4.33	-3.90
wtr-stk	DT -c deg C	1.58	2.39	2.44	2.09	2.10	2.44	2.13	2.43	2.49
piston vel	(m/s)	0.63	0.86	0.94	0.81	0.80	0.89	0.79	0.93	0.85
pdr phase		139.61	141.13	137.75	140.77	142.22	142.75	144.43	139.52	148.68
Tavgh	degC	24.48	24.65	24.60	24.47	24.49	24.58	24.56	24.63	24.77
Tavgc	degC	24.21	24.31	24.26	24.09	24.10	24.17	24.14	24.19	24.31
Mtbh	degC	27.64	29.01	29.09	28.62	28.68	28.95	28.49	28.79	28.47
Mtbc	degC	27.48	28.97	29.03	28.53	28.56	28.90	28.34	28.69	28.30
Inbal/(Qc+Wac)*100		17.90	15.09	17.33	9.92	3.63	4.90	12.21	15.41	20.08
GBS1-h	degC	26.98	28.08	28.14	27.77	27.85	28.11	27.75	28.02	27.77
GBS2-h	degC	27.64	28.86	28.94	28.53	28.57	28.81	28.41	28.65	28.35
GBS3-h	degC	27.64	29.01	29.09	28.62	28.68	28.95	28.49	28.79	28.47
GBS1-c	degC	22.46	21.87	21.80	21.94	21.92	21.67	21.87	21.65	21.66
GBS2-c	degC	22.44	21.49	21.39	21.66	21.67	21.33	21.73	21.42	21.55
GBS3-c	degC	22.28	21.45	21.34	21.57	21.55	21.28	21.58	21.32	21.38
Hot Stack Avg	degC	27.35	28.54	28.62	28.22	28.27	28.53	28.13	28.40	28.12
Cold Stack Avg	degC	22.37	21.54	21.44	21.67	21.66	21.36	21.69	21.41	21.49

Key to Notation

D-temperature difference
i-in
o-out
h-hot
c-cold
M-metal
tb-tube
f-fin
G-gas
B-between
F-fins
D-duct side

S-stack side
38-3/8" off of the heat exchanger
C-center of heat exchanger
Q-quarter diameter of heat exchanger
Wac-acoustic power
Qc, Qh – heat transferred
V-volumetric flow rate
p0-pressure at driver
wtr-stk – temp diff between water and stack
GBS1-3 – temp of gas stack for area ratio

Appendix II: Table of Thermoacoustic Results for the Microchannel Heat Exchangers

Hot Exchanger Results

Data Point	Acoustic Information and Calculation							Water Flow in HX Tubes Calculation				
	u est	urms	ReD	LMTD	UA	h air side	j air side	H20 vel 1 channel	ReD	friction factor	Nusselt	htubes
1	2.94	2.08	1727.93	3.03	57.84	781.61	0.0180	1.0340	1890.28	0.0536	10.43	3737.02
2	2.38	1.68	1399.99	2.53	57.34	764.21	0.0217	1.0340	1886.91	0.0536	10.41	3729.39
3	1.32	0.94	777.91	1.59	59.87	879.83	0.0450	1.0340	1881.68	0.0537	10.38	3717.03
4	3.78	2.68	2222.97	3.60	64.00	1091.46	0.0195	1.0340	1900.12	0.0535	10.45	3745.72
5	2.41	1.70	2110.29	2.26	58.13	797.97	0.0150	1.0340	1888.37	0.0536	10.40	3724.96
6	3.39	2.40	2968.31	3.09	63.15	1045.40	0.0140	1.0340	1895.19	0.0535	10.43	3736.56
7	3.81	2.69	3336.38	3.44	65.32	1183.28	0.0141	1.0340	1899.24	0.0535	10.44	3742.46
8	3.96	2.80	4611.24	2.83	63.56	1073.96	0.0130	1.0322	1886.36	0.0536	10.42	3731.35
9	3.96	2.80	4611.24	3.52	64.42	1123.59	0.0136	1.0322	1892.00	0.0536	10.44	3739.49
10	3.64	2.57	2852.70	2.79	66.68	1305.63	0.0257	1.0251	1880.79	0.0537	10.39	3721.88
11	3.73	2.64	2927.90	3.70	66.01	1242.21	0.0238	1.0251	1887.37	0.0536	10.41	3733.03
12	3.17	2.24	4312.61	2.13	65.46	1217.31	0.0191	1.0251	1870.63	0.0538	10.37	3714.03
13	3.61	2.55	4916.04	2.55	65.47	1213.35	0.0167	1.0251	1875.09	0.0537	10.38	3719.53
14	4.35	3.08	5926.56	3.11	64.34	1128.16	0.0129	1.0251	1878.95	0.0537	10.40	3726.16
15	4.47	3.16	6091.71	3.36	65.62	1215.88	0.0135	1.0251	1881.72	0.0537	10.41	3729.52
16	3.83	2.71	4373.16	2.90	64.42	1135.43	0.0176	1.0251	1880.54	0.0537	10.39	3723.62
17	4.35	3.08	4963.08	3.35	66.72	1301.15	0.0178	1.0251	1885.78	0.0536	10.40	3729.75
18	3.55	2.51	2086.36	3.39	67.49	1364.08	0.0260	1.0251	1885.91	0.0536	10.41	3731.75
19	3.76	2.66	2207.34	3.58	68.91	1493.17	0.0269	1.0251	1887.61	0.0536	10.42	3734.35
20	0.42	0.30	403.84	0.93	53.63	625.72	0.0713	1.0746	1930.78	0.0532	10.51	3758.45
21	0.54	0.38	522.43	1.91	68.48	1410.00	0.1241	1.0746	1943.40	0.0530	10.53	3769.97
22	0.73	0.51	531.01	1.54	73.13	1942.63	0.1454	1.0746	1940.94	0.0531	10.53	3768.28
23	0.71	0.50	520.47	1.12	70.34	1606.08	0.1226	1.0746	1937.13	0.0531	10.51	3761.12
24	2.37	1.67	2397.83	1.88	65.32	1114.04	0.0208	1.1312	2043.48	0.0521	10.71	3833.50
25	2.85	2.01	2881.95					1.1312	2047.12	0.0521	10.73	3838.70
26	1.01	0.71	1077.57	0.92	56.59	705.02	0.0309	1.1312	2040.99	0.0521	10.69	3826.27
27	2.08	1.47	2230.11	1.53	69.45	1429.07	0.0302	1.1312	2050.56	0.0520	10.70	3830.91
28	0.78	0.55	679.41	0.96	70.32	1515.69	0.0885	1.1312	2045.97	0.0521	10.69	3826.70
29	0.94	0.67	689.42	0.92	69.36	1425.20	0.0822	1.1312	2053.73	0.0520	10.69	3827.04
30	2.32	1.64	2827.18	1.64	63.80	1023.85	0.0184	1.1312	2049.52	0.0520	10.71	3832.01
31	1.08	0.76	1317.32	0.93	65.17	1110.77	0.0428	1.1312	2042.06	0.0521	10.69	3824.89
32	1.82	1.29	1069.47	2.86	35.33	273.60	0.0102	0.8661	1631.26	0.0566	9.82	3528.31
33	3.04	2.15	1785.45	3.87	42.78	393.75	0.0088	0.8661	1622.48	0.0567	9.88	3549.22
34	3.08	2.18	1808.25	3.99	41.52	370.09	0.0081	0.8661	1620.67	0.0567	9.89	3550.50
35	2.62	1.86	1541.84	3.73	40.39	350.92	0.0091	0.8661	1630.89	0.0566	9.85	3540.62
36	2.61	1.85	1534.20	3.76	46.26	458.76	0.0119	0.9191	1731.79	0.0553	10.05	3611.92
37	2.73	1.93	1601.42	3.92	50.31	558.74	0.0139	0.9191	1719.13	0.0555	10.08	3619.91
38	2.10	1.49	1234.29	3.55	50.49	564.95	0.0182	0.9191	1718.07	0.0555	10.06	3614.18
39	1.98	1.40	1164.49	3.74	53.87	670.68	0.0229	0.9191	1721.02	0.0555	10.07	3617.46
40	1.67	1.18	979.75	3.32	58.71	873.53	0.0355	0.9191	1726.38	0.0554	10.06	3612.55

Cold Exchanger Results

Data Point	Acoustic Information and Calculation							Water Flow in HX Tubes Calculation				
	u est	urms	ReD	LMTD	UA	h air side	j air side	H20 vel 1 channel	ReD	friction factor	Nusselt	htubes
1	3.93	2.78	3143.17	3.06	35.85	277.50	0.0040	0.8484	1542.77	0.0578	9.59	3590.10
2	3.18	2.25	2508.04	2.53	36.00	279.52	0.0050	0.8484	1540.64	0.0578	9.59	3591.03
3	1.80	1.27	1379.26	1.72	36.09	280.68	0.0091	0.8484	1537.36	0.0579	9.60	3592.46
4	5.00	3.54	3942.66	3.51	36.05	280.43	0.0032	0.8484	1546.50	0.0577	9.59	3588.48
5	3.22	2.28	3808.57	2.05	31.28	220.18	0.0026	0.8484	1539.37	0.0578	9.59	3591.59
6	4.51	3.19	5354.89	2.69	32.96	240.10	0.0020	0.8484	1541.41	0.0578	9.59	3590.69
7	5.06	3.57	6004.04	2.93	33.96	252.59	0.0019	0.8484	1542.67	0.0578	9.59	3590.14
8	4.93	3.49	7313.49	2.52	33.70	247.19	0.0021	0.8837	1601.42	0.0570	9.73	3641.68
9	4.93	3.49	7313.49	3.00	34.21	253.54	0.0021	0.8837	1603.72	0.0570	9.73	3640.70
10	4.55	3.22	4496.44	2.78	37.60	295.59	0.0041	0.9368	1705.57	0.0557	9.91	3709.81
11	4.65	3.29	4598.59	3.42	37.24	290.58	0.0039	0.9368	1708.12	0.0556	9.91	3708.77

12	3.98	2.81	6974.17	1.86	34.11	249.33	0.0027	0.9368	1696.37	0.0558	9.92	3713.57
13	4.54	3.21	7992.87	2.18	34.44	253.50	0.0024	0.9368	1698.59	0.0557	9.92	3712.66
14	5.47	3.87	9687.30	2.57	33.93	247.24	0.0019	0.9368	1700.02	0.0557	9.92	3712.08
15	5.62	3.97	9926.58	2.71	34.12	249.49	0.0019	0.9368	1701.08	0.0557	9.92	3711.64
16	4.82	3.41	7078.00	2.47	34.56	255.03	0.0027	0.9368	1703.24	0.0557	9.91	3710.76
17	5.49	3.88	8089.85	2.85	33.79	245.55	0.0023	0.9368	1705.18	0.0557	9.91	3709.97
18	4.65	3.29	3623.29	3.00	36.69	282.53	0.0035	0.9421	1714.97	0.0555	9.93	3716.90
19	4.91	3.47	3813.80	3.16	36.91	285.65	0.0034	0.9421	1716.30	0.0555	9.93	3716.36
20	0.65	0.46	660.87	0.91	43.15	403.98	0.0287	0.7954	1425.80	0.0596	9.41	3523.10
21	0.75	0.53	805.89	2.10	41.25	367.91	0.0219	0.7954	1433.35	0.0594	9.40	3519.63
22	0.96	0.68	792.95	1.53	40.35	351.90	0.0185	0.7954	1430.43	0.0595	9.41	3520.97
23	0.95	0.67	767.78	1.12	38.63	323.00	0.0174	0.7954	1428.73	0.0595	9.41	3521.75
24	3.13	2.21	4254.54	2.05	40.30	346.65	0.0041	0.8307	1495.67	0.0585	9.54	3571.63
25	3.73	2.64	5041.56	2.31	40.12	343.66	0.0034	0.8307	1494.60	0.0585	9.54	3572.11
26	1.37	0.97	1869.69	0.97	42.40	384.21	0.0108	0.8307	1495.71	0.0585	9.54	3571.62
27	2.72	1.92	3844.71	1.68	41.62	370.15	0.0051	0.8307	1501.07	0.0584	9.53	3569.23
28	1.02	0.72	1018.75	0.93	40.91	357.38	0.0147	0.8307	1497.47	0.0585	9.54	3570.83
29	1.24	0.88	1069.48	1.03	46.20	460.05	0.0183	0.8484	1536.23	0.0579	9.60	3592.96
30	3.00	2.12	4844.67	1.72	39.04	324.34	0.0038	0.8484	1531.71	0.0580	9.60	3594.94
31	1.46	1.03	2320.81	0.91	37.15	295.48	0.0072	0.8484	1526.81	0.0580	9.61	3597.09
32	2.40	1.70	1835.47	1.83	40.94	373.83	0.0091	0.7335	1371.76	0.0605	9.09	3402.17
33	3.98	2.81	3088.34	2.75	39.38	345.43	0.0050	0.7335	1375.28	0.0604	9.08	3400.53
34	4.04	2.86	3152.64	2.81	38.65	332.71	0.0047	0.7335	1373.63	0.0604	9.09	3401.30
35	3.44	2.43	2670.25	2.40	38.16	324.22	0.0054	0.7335	1367.22	0.0605	9.09	3404.30
36	3.42	2.42	2651.76	2.42	37.98	323.04	0.0054	0.7194	1341.25	0.0610	9.03	3382.10
37	3.57	2.52	2779.43	2.79	36.45	298.74	0.0048	0.7194	1343.85	0.0609	9.03	3380.86
38	2.75	1.95	2133.71	2.44	37.03	307.76	0.0064	0.7194	1342.71	0.0610	9.03	3381.40
39	2.62	1.85	2054.57	2.76	35.45	283.57	0.0062	0.7194	1344.60	0.0609	9.03	3380.51
40	2.18	1.54	1685.09	2.81	32.89	248.21	0.0066	0.7194	1348.95	0.0609	9.03	3378.45

Uest' - estimated particle velocity from DELTAE, (m/s)

urms - root mean square velocity, (m/s)

ReD - Reynolds number based on hydraulic diameter

LMTD - Log Mean Temperature Difference, (K)

h air side - heat transfer coefficient on air side, $(W/m^2 K)$

j air side – j-Colburn factor on the air side

H20 vel 1 channel – velocity of water in one heat exchanger channel

Nusselt – Nusselt number for water

htubes – heat transfer coefficient for water in tubes

Appendix III: Table of Thermoacoustic He-Ar Properties

Hot Exchanger Properties

Data Point	rho	k	mu	DeltaK	DeltaN	Pr	Cp	beta	gamma	part displace	Hxfer Area	P	Dh	ReD	Hxref Area based on pd
							Thermoacoustic Working Fluid Properties								
1	11.03	0.0613	0.000024	0.000100	0.000063	0.40	1030.0	0.0033	1.6667	0.0027	0.2307	0.0160	0.0018	1727.93	0.0680
2	11.03	0.0613	0.000024	0.000100	0.000063	0.40	1030.0	0.0033	1.6667	0.0022	0.2307	0.0160	0.0018	1399.99	0.0553
3	11.03	0.0613	0.000024	0.000100	0.000063	0.40	1030.0	0.0033	1.6667	0.0012	0.2307	0.0160	0.0018	777.91	0.0313
4	11.03	0.0613	0.000024	0.000100	0.000063	0.40	1030.0	0.0033	1.6667	0.0035	0.2307	0.0160	0.0018	2222.97	0.0871
5	16.54	0.0613	0.000024	0.000081	0.000052	0.40	1030.0	0.0033	1.6667	0.0022	0.2307	0.0160	0.0018	2110.29	0.0556
6	16.54	0.0613	0.000024	0.000081	0.000052	0.40	1030.0	0.0033	1.6667	0.0031	0.2307	0.0160	0.0018	2968.31	0.0777
7	16.54	0.0613	0.000024	0.000081	0.000052	0.40	1030.0	0.0033	1.6667	0.0035	0.2307	0.0160	0.0018	3336.38	0.0872
8	22.58	0.0425	0.000025	0.000074	0.000049	0.44	754.5	0.0033	1.6667	0.0044	0.2307	0.0160	0.0018	4611.24	0.1086
9	22.58	0.0425	0.000025	0.000074	0.000049	0.44	754.5	0.0033	1.6667	0.0044	0.2307	0.0160	0.0018	4611.24	0.1085
10	15.06	0.0423	0.000024	0.000091	0.000060	0.44	754.5	0.0033	1.6667	0.0040	0.2307	0.0160	0.0018	2852.70	0.0999
11	15.06	0.0423	0.000024	0.000091	0.000060	0.44	754.5	0.0033	1.6667	0.0041	0.2307	0.0160	0.0018	2927.90	0.1024
12	26.39	0.0344	0.000025	0.000069	0.000047	0.46	645.8	0.0033	1.6667	0.0038	0.2307	0.0160	0.0018	4312.61	0.0938
13	26.39	0.0344	0.000025	0.000069	0.000047	0.46	645.8	0.0033	1.6667	0.0043	0.2307	0.0160	0.0018	4916.04	0.1067
14	26.39	0.0344	0.000025	0.000069	0.000047	0.46	645.8	0.0033	1.6667	0.0052	0.2307	0.0160	0.0018	5926.56	0.1283
15	26.39	0.0344	0.000025	0.000069	0.000047	0.46	645.8	0.0033	1.6667	0.0053	0.2307	0.0160	0.0018	6091.71	0.1319
16	21.99	0.0343	0.000025	0.000076	0.000052	0.46	645.8	0.0033	1.6667	0.0046	0.2307	0.0160	0.0018	4373.16	0.1133
17	21.99	0.0343	0.000025	0.000076	0.000051	0.46	645.8	0.0033	1.6667	0.0052	0.2307	0.0160	0.0018	4963.08	0.1282
18	11.03	0.0613	0.000024	0.000101	0.000064	0.40	1030.0	0.0033	1.6667	0.0034	0.2307	0.0160	0.0018	2086.36	0.0836
19	11.03	0.0613	0.000024	0.000101	0.000064	0.40	1030.0	0.0033	1.6667	0.0035	0.2307	0.0160	0.0018	2207.34	0.0883
20	18.51	0.0524	0.000024	0.000079	0.000051	0.42	896.0	0.0033	1.6667	0.0004	0.2307	0.0160	0.0018	403.84	0.0113
21	18.51	0.0524	0.000024	0.000079	0.000051	0.42	896.0	0.0033	1.6667	0.0005	0.2307	0.0160	0.0018	522.43	0.0144
22	13.79	0.0613	0.000024	0.000090	0.000057	0.40	1030.0	0.0033	1.6667	0.0007	0.2307	0.0160	0.0018	531.01	0.0179
23	13.79	0.0613	0.000024	0.000090	0.000057	0.40	1030.0	0.0033	1.6667	0.0007	0.2307	0.0160	0.0018	520.47	0.0176
24	19.38	0.0538	0.000024	0.000077	0.000050	0.41	917.3	0.0033	1.6667	0.0023	0.2307	0.0160	0.0018	2397.83	0.0582
25	19.38	0.0538	0.000024	0.000077	0.000050	0.41	917.3	0.0033	1.6667	0.0028	0.2307	0.0160	0.0018	2881.95	0.0697
26	20.59	0.0509	0.000024	0.000075	0.000049	0.42	874.3	0.0033	1.6667	0.0010	0.2307	0.0160	0.0018	1077.57	0.0257
27	20.59	0.0509	0.000024	0.000075	0.000049	0.42	874.3	0.0033	1.6667	0.0021	0.2307	0.0160	0.0018	2230.11	0.0522
28	16.54	0.0613	0.000024	0.000082	0.000052	0.40	1030.0	0.0033	1.6667	0.0007	0.2307	0.0160	0.0018	679.41	0.0190
29	13.79	0.0613	0.000024	0.000090	0.000057	0.40	1030.0	0.0033	1.6667	0.0009	0.2307	0.0160	0.0018	689.42	0.0228
30	23.63	0.0470	0.000025	0.000072	0.000047	0.43	817.4	0.0033	1.6667	0.0025	0.2307	0.0160	0.0018	2827.18	0.0618
31	23.63	0.0470	0.000025	0.000072	0.000047	0.43	817.4	0.0033	1.6667	0.0011	0.2307	0.0160	0.0018	1317.32	0.0292
32	11.03	0.0613	0.000024	0.000101	0.000064	0.40	1030.0	0.0033	1.6667	0.0017	0.2307	0.0160	0.0018	1069.47	0.0431
33	11.03	0.0613	0.000024	0.000101	0.000064	0.40	1030.0	0.0033	1.6667	0.0028	0.2307	0.0160	0.0018	1785.45	0.0712
34	11.03	0.0613	0.000024	0.000101	0.000064	0.40	1030.0	0.0033	1.6667	0.0029	0.2307	0.0160	0.0018	1808.25	0.0720
35	11.03	0.0613	0.000024	0.000101	0.000064	0.40	1030.0	0.0033	1.6667	0.0025	0.2307	0.0160	0.0018	1541.84	0.0616
36	11.03	0.0613	0.000024	0.000101	0.000064	0.40	1030.0	0.0033	1.6667	0.0024	0.2307	0.0160	0.0018	1534.20	0.0613
37	11.03	0.0613	0.000024	0.000101	0.000064	0.40	1030.0	0.0033	1.6667	0.0026	0.2307	0.0160	0.0018	1601.42	0.0640
38	11.03	0.0613	0.000024	0.000101	0.000064	0.40	1030.0	0.0033	1.6667	0.0020	0.2307	0.0160	0.0018	1234.29	0.0496
39	11.03	0.0613	0.000024	0.000101	0.000064	0.40	1030.0	0.0033	1.6667	0.0019	0.2307	0.0160	0.0018	1164.49	0.0468
40	11.03	0.0613	0.000024	0.000101	0.000064	0.40	1030.0	0.0033	1.6667	0.0016	0.2307	0.0160	0.0018	979.75	0.0397

Cold Exchanger Properties

Data Point	rho	k	mu	DeltaK	DeltaN	Pr	Cp	beta	gamma	part displace	Hxfer Area	P	Dh	ReD	Hxref Area based on pd
							Thermoacoustic Working Fluid Properties								
1	13.13	0.0540	0.000021	0.000086	0.000054	0.40	1030.0	0.0039	1.6667	0.0036	0.2307	0.0160	0.0018	3143.17	0.0904
2	13.01	0.0543	0.000021	0.000087	0.000055	0.40	1030.0	0.0039	1.6667	0.0029	0.2307	0.0160	0.0018	2508.04	0.0735
3	12.81	0.0550	0.000021	0.000088	0.000055	0.40	1030.0	0.0038	1.6667	0.0017	0.2307	0.0160	0.0018	1379.26	0.0421
4	13.02	0.0543	0.000021	0.000087	0.000055	0.40	1030.0	0.0039	1.6667	0.0046	0.2307	0.0160	0.0018	3942.66	0.1148
5	19.60	0.0542	0.000021	0.000070	0.000044	0.40	1030.0	0.0039	1.6667	0.0030	0.2307	0.0160	0.0018	3808.57	0.0738
6	19.65	0.0541	0.000021	0.000070	0.000044	0.40	1030.0	0.0039	1.6667	0.0041	0.2307	0.0160	0.0018	5354.89	0.1029
7	19.65	0.0541	0.000021	0.000070	0.000044	0.40	1030.0	0.0039	1.6667	0.0046	0.2307	0.0160	0.0018	6004.04	0.1152
8	25.81	0.0384	0.000022	0.000066	0.000044	0.43	754.5	0.0038	1.6667	0.0055	0.2307	0.0160	0.0018	7313.49	0.1351
9	25.81	0.0384	0.000022	0.000066	0.000044	0.43	754.5	0.0038	1.6667	0.0054	0.2307	0.0160	0.0018	7313.49	0.1349
10	17.12	0.0385	0.000022	0.000081	0.000053	0.43	754.5	0.0037	1.6667	0.0050	0.2307	0.0160	0.0018	4496.44	0.1247
11	17.13	0.0384	0.000022	0.000081	0.000053	0.43	754.5	0.0037	1.6667	0.0051	0.2307	0.0160	0.0018	4598.59	0.1271
12	30.32	0.0309	0.000022	0.000061	0.000042	0.46	645.8	0.0038	1.6667	0.0047	0.2307	0.0160	0.0018	6974.17	0.1174

13	30.39	0.0308	0.000022	0.000061	0.000041	0.46	645.8	0.0038	1.6667	0.0054	0.2307	0.0160	0.0018	7992.87	0.1337
14	30.46	0.0308	0.000022	0.000061	0.000041	0.46	645.8	0.0038	1.6667	0.0065	0.2307	0.0160	0.0018	9687.30	0.1610
15	30.44	0.0308	0.000022	0.000061	0.000041	0.46	645.8	0.0038	1.6667	0.0067	0.2307	0.0160	0.0018	9926.58	0.1653
16	25.24	0.0308	0.000022	0.000067	0.000045	0.46	645.8	0.0038	1.6667	0.0057	0.2307	0.0160	0.0018	7078.00	0.1422
17	25.31	0.0308	0.000022	0.000067	0.000045	0.46	645.8	0.0038	1.6667	0.0065	0.2307	0.0160	0.0018	8089.85	0.1613
18	12.93	0.0546	0.000021	0.000088	0.000056	0.40	1030.0	0.0039	1.6667	0.0044	0.2307	0.0160	0.0018	3623.29	0.1091
19	12.91	0.0546	0.000021	0.000088	0.000056	0.40	1030.0	0.0039	1.6667	0.0046	0.2307	0.0160	0.0018	3813.80	0.1151
20	19.02	0.0513	0.000024	0.000077	0.000050	0.42	896.0	0.0034	1.6667	0.0006	0.2307	0.0160	0.0018	660.87	0.0170
21	19.61	0.0502	0.000023	0.000075	0.000049	0.42	896.0	0.0035	1.6667	0.0007	0.2307	0.0160	0.0018	805.89	0.0196
22	14.75	0.0584	0.000023	0.000085	0.000054	0.40	1030.0	0.0035	1.6667	0.0009	0.2307	0.0160	0.0018	792.95	0.0233
23	14.60	0.0588	0.000023	0.000085	0.000054	0.40	1030.0	0.0035	1.6667	0.0009	0.2307	0.0160	0.0018	767.78	0.0230
24	22.86	0.0477	0.000021	0.000067	0.000043	0.41	917.3	0.0039	1.6667	0.0031	0.2307	0.0160	0.0018	4254.54	0.0766
25	22.80	0.0478	0.000021	0.000067	0.000043	0.41	917.3	0.0039	1.6667	0.0037	0.2307	0.0160	0.0018	5041.56	0.0910
26	23.62	0.0460	0.000022	0.000067	0.000043	0.42	874.3	0.0038	1.6667	0.0014	0.2307	0.0160	0.0018	1869.69	0.0345
27	24.05	0.0454	0.000022	0.000066	0.000042	0.42	874.3	0.0038	1.6667	0.0027	0.2307	0.0160	0.0018	3844.71	0.0678
28	17.82	0.0581	0.000023	0.000077	0.000049	0.40	1030.0	0.0036	1.6667	0.0010	0.2307	0.0160	0.0018	1018.75	0.0246
29	15.13	0.0573	0.000022	0.000083	0.000052	0.40	1030.0	0.0036	1.6667	0.0012	0.2307	0.0160	0.0018	1069.48	0.0296
30	27.59	0.0419	0.000022	0.000063	0.000041	0.43	817.4	0.0038	1.6667	0.0032	0.2307	0.0160	0.0018	4844.67	0.0798
31	27.37	0.0421	0.000022	0.000063	0.000041	0.43	817.4	0.0038	1.6667	0.0015	0.2307	0.0160	0.0018	2320.81	0.0391
32	12.80	0.0550	0.000021	0.000088	0.000056	0.40	1030.0	0.0038	1.6667	0.0023	0.2307	0.0160	0.0018	1835.47	0.0565
33	12.91	0.0546	0.000021	0.000088	0.000055	0.40	1030.0	0.0039	1.6667	0.0037	0.2307	0.0160	0.0018	3088.34	0.0928
34	12.94	0.0545	0.000021	0.000088	0.000055	0.40	1030.0	0.0039	1.6667	0.0038	0.2307	0.0160	0.0018	3152.64	0.0941
35	12.91	0.0547	0.000021	0.000088	0.000055	0.40	1030.0	0.0039	1.6667	0.0032	0.2307	0.0160	0.0018	2670.25	0.0805
36	12.90	0.0547	0.000021	0.000088	0.000055	0.40	1030.0	0.0039	1.6667	0.0032	0.2307	0.0160	0.0018	2651.76	0.0800
37	12.93	0.0546	0.000021	0.000088	0.000055	0.40	1030.0	0.0039	1.6667	0.0033	0.2307	0.0160	0.0018	2779.43	0.0834
38	12.90	0.0547	0.000021	0.000088	0.000055	0.40	1030.0	0.0039	1.6667	0.0026	0.2307	0.0160	0.0018	2133.71	0.0646
39	12.99	0.0544	0.000021	0.000087	0.000055	0.40	1030.0	0.0039	1.6667	0.0025	0.2307	0.0160	0.0018	2054.57	0.0614
40	12.88	0.0547	0.000021	0.000088	0.000056	0.40	1030.0	0.0038	1.6667	0.0020	0.2307	0.0160	0.0018	1685.09	0.0514

rho – density, (kg/m^3)

k – heat transfer coefficient, (W/m-K)

mu – dynamic viscosity, (N-s/m^2)

DeltaK – thermal penetration depth, (m)

DeltaN – viscous penetration depth, (m)

Pr – Prandtl number

Cp – specific heat, (J/kg-K)

beta – thermal expansion coefficient, (K^{-1})

gamma – ratio of specific heats

part displace – particle displacement, (m)

P – perimeter of heat exchanger fin, (m)

Dh – hydraulic diameter of heat exchanger, (m)

Appendix IV: Table of Water-Side Properties

Hot Exchanger Properties

Data Point	water properties					
	mu	mu(s)	density	cp	k	Pr
1	0.000926	0.000868	997.74	4180.19	0.61	6.37
2	0.000928	0.000881	997.75	4180.23	0.61	6.38
3	0.000931	0.000904	997.77	4180.30	0.61	6.40
4	0.000922	0.000851	997.70	4180.07	0.61	6.33
5	0.000927	0.000888	997.74	4180.22	0.61	6.37
6	0.000924	0.000867	997.72	4180.13	0.61	6.35
7	0.000922	0.000856	997.70	4180.08	0.61	6.33
8	0.000927	0.000874	997.74	4180.20	0.61	6.37
9	0.000924	0.000859	997.72	4180.13	0.61	6.35
10	0.000923	0.000873	997.71	4180.11	0.61	6.34
11	0.000920	0.000853	997.68	4180.03	0.61	6.32
12	0.000928	0.000889	997.75	4180.24	0.61	6.38
13	0.000926	0.000879	997.73	4180.18	0.61	6.36
14	0.000924	0.000867	997.72	4180.13	0.61	6.35
15	0.000923	0.000860	997.70	4180.10	0.61	6.34
16	0.000923	0.000870	997.71	4180.11	0.61	6.34
17	0.000921	0.000859	997.69	4180.05	0.61	6.32
18	0.000921	0.000855	997.69	4180.05	0.61	6.32
19	0.000920	0.000851	997.68	4180.03	0.61	6.32
20	0.000943	0.000923	997.87	4180.60	0.61	6.49
21	0.000937	0.000899	997.82	4180.44	0.61	6.45
22	0.000938	0.000903	997.83	4180.47	0.61	6.46
23	0.000940	0.000916	997.84	4180.52	0.61	6.47
24	0.000938	0.000902	997.83	4180.47	0.61	6.45
25	0.000936	0.000893	997.81	4180.43	0.61	6.44
26	0.000939	0.000915	997.84	4180.50	0.61	6.46
27	0.000934	0.000905	997.80	4180.39	0.61	6.43
28	0.000936	0.000913	997.82	4180.44	0.61	6.45
29	0.000933	0.000910	997.79	4180.35	0.61	6.42
30	0.000935	0.000903	997.80	4180.40	0.61	6.43
31	0.000938	0.000917	997.83	4180.49	0.61	6.46
32	0.000899	0.000842	997.51	4179.51	0.61	6.15
33	0.000904	0.000813	997.48	4179.94	0.61	6.20
34	0.000905	0.000812	997.49	4179.96	0.61	6.21
35	0.000899	0.000821	997.51	4179.52	0.61	6.16
36	0.000899	0.000820	997.51	4179.50	0.61	6.15
37	0.000905	0.000814	997.49	4179.97	0.61	6.21
38	0.000906	0.000824	997.50	4179.98	0.61	6.22
39	0.000904	0.000818	997.48	4179.95	0.61	6.20
40	0.000901	0.000824	997.45	4179.89	0.61	6.18

Cold Exchanger Properties

Data Point	Water Properties					
	mu	mu(s)	density	cp	k	Pr
1	0.000931	0.000994	997.78	4180.32	0.61	6.41
2	0.000933	0.000994	997.79	4180.35	0.61	6.42
3	0.000935	0.000994	997.80	4180.40	0.61	6.43
4	0.000929	0.000994	997.76	4180.26	0.61	6.39
5	0.000933	0.000994	997.79	4180.37	0.61	6.42
6	0.000932	0.000994	997.78	4180.34	0.61	6.41
7	0.000931	0.000994	997.78	4180.32	0.61	6.41
8	0.000935	0.000994	997.80	4180.40	0.61	6.43
9	0.000933	0.000994	997.79	4180.36	0.61	6.42
10	0.000930	0.000994	997.77	4180.29	0.61	6.40
11	0.000929	0.000994	997.76	4180.25	0.61	6.39
12	0.000935	0.000994	997.81	4180.41	0.61	6.44
13	0.000934	0.000994	997.80	4180.38	0.61	6.43

	mu	mu(s)	density	Cp	k	Pr
14	0.000933	0.000994	997.79	4180.36	0.61	6.42
15	0.000933	0.000994	997.79	4180.35	0.61	6.42
16	0.000932	0.000994	997.78	4180.32	0.61	6.41
17	0.000930	0.000994	997.77	4180.29	0.61	6.40
18	0.000930	0.000994	997.77	4180.29	0.61	6.40
19	0.000930	0.000994	997.76	4180.27	0.61	6.39
20	0.000945	0.000994	997.89	4180.65	0.61	6.51
21	0.000940	0.000994	997.85	4180.53	0.61	6.47
22	0.000942	0.000994	997.86	4180.57	0.61	6.49
23	0.000943	0.000994	997.87	4180.60	0.61	6.50
24	0.000941	0.000994	997.85	4180.55	0.61	6.48
25	0.000941	0.000994	997.86	4180.57	0.61	6.48
26	0.000941	0.000994	997.85	4180.55	0.61	6.48
27	0.000937	0.000994	997.83	4180.46	0.61	6.45
28	0.000940	0.000994	997.84	4180.52	0.61	6.47
29	0.000935	0.000994	997.81	4180.41	0.61	6.44
30	0.000938	0.000994	997.83	4180.48	0.61	6.46
31	0.000941	0.000994	997.86	4180.56	0.61	6.48
32	0.000905	0.000994	997.56	4179.67	0.61	6.20
33	0.000903	0.000994	997.54	4179.62	0.61	6.19
34	0.000904	0.000994	997.55	4179.64	0.61	6.19
35	0.000909	0.000994	997.59	4179.75	0.61	6.23
36	0.000908	0.000994	997.59	4179.74	0.61	6.23
37	0.000906	0.000994	997.57	4179.70	0.61	6.21
38	0.000907	0.000994	997.58	4179.72	0.61	6.22
39	0.000906	0.000994	997.57	4179.69	0.61	6.21
40	0.000903	0.000994	997.54	4179.61	0.61	6.19

mu – dynamic viscosity, (N-s/m^2)

mu(s) – dynamic viscosity at surface of fluid, (N-s/m^2)

density – density, (kg/m^3)

k – heat transfer coefficient, (W/m-K)

Cp – specific heat, (J/kg-K)

Pr – Prandtl number

Appendix V: Table of Thermoacoustic Raw Data for the Microchannel Heat Exchangers

Measurement	Units	Data Points		
		1	2	3
pressure	psi	86	157	86
Mix		0.55	0.55	0.55
Freq	Hz	172.90	174.00	172.70
Wac	W	20.70	44.00	45.60
Qc	W	23.60	29.00	65.20
Qh	W	47.30	80.50	121.90
DTh	degC	0.39	0.22	0.80
DTc	degC	0.31	0.15	0.62
Vrateh	L/min	4.60	5.20	2.19
Vratec	L/min	3.00	2.70	1.50
stack DT	degC	2.44	7.06	6.52
p0	kPa	12.20	26.20	18.80
Qc+Wac-Qh	balance	-3.00	-7.50	-11.10
Thi	degC	22.22	24.39	20.78
Tci	degC	25.06	24.56	26.28
wtr-stk	DT -h deg C	-2.39	-3.94	-6.28
wtr-stk	DT -c deg C	2.91	3.28	5.78
piston vel	(m/s)	0.51	0.60	0.82
pdr phase		167.00	145.70	153.00
Tavgh	degC	22.42	24.50	21.18
Tavgc	degC	25.21	24.63	26.59
Inbal/(Qc+Wac)*100		6.77	10.27	10.02

Appendix VI: Table of Thermoacoustic Results for the Microchannel Heat Exchangers

Hot Exchanger Results

Data Point	Acoustic Information and Calculation							Water Flow in HX Tubes Calculation				
	u est	urms	ReD	LMTD	UA	h air side	j air side	H20 vel 1 channel	ReD	friction factor	Nusselt	htubes
1	1.48	1.05	530.27	2.19	21.61	198.46	0.0211	0.33	3456.42	0.04	22.13	2084.31
2	1.60	1.13	1045.17	3.83	21.01	151.19	0.0081	0.37	3907.26	0.04	25.46	2398.21
3	2.16	1.53	775.19	5.87	20.77	212.79	0.0154	0.16	1645.56	0.06	20.00	1883.91

Cold Exchanger Properties

	u est	urms	ReD	LMTD	UA	h air side	j air side	H20 vel 1 channel	ReD	friction factor	Nusselt	htubes
1	1.95	1.38	817.26	3.06	7.71	39.81	0.0029	0.22	2254.19	0.05	12.51	1178.77
2	2.11	1.49	1751.68	3.35	8.65	56.69	0.0020	0.19	2028.77	0.05	10.54	992.56

Appendix VII: Table of Thermoacoustic He-Ar Properties

Hot Exchanger Results

Data Point	Thermoacoustic Working Fluid Properties							beta	gamma	part displace	Hxfer Area	P	Dh	ReD	Hxref Area based on pd
	rho	k	mu	DeltaK	DeltaN	Pr	Cp								
1	4.74	0.0612	0.000024	0.000152	0.000096	0.3988	1030		1.6667	0.0014	0.3355	0.0255	0.0025	530.27	0.0371
2	8.66	0.0612	0.000024	0.000112	0.000071	0.4005	1030		1.6667	0.0015	0.3355	0.0255	0.0025	1045.17	0.0399
3	4.74	0.0612	0.000024	0.000152	0.000096	0.3988	1030		1.6667	0.0020	0.3355	0.0255	0.0025	775.19	0.0536

Cold Exchanger Properties

Data Point	Thermoacoustic Working Fluid Properties							beta	gamma	part displace	Hxfer Area	P	Dh	ReD	Hxref Area based on pd
	rho	k	mu	DeltaK	DeltaN	Pr	Cp								
1	5.17	0.0575	0.000022	0.000141	0.000089	0.3975	1030		1.6667	0.0018	0.3355	0.0255	0.0025	817.26	0.0486
2	9.92	0.0555	0.000021	0.000100	0.000063	0.3981	1030		1.6667	0.0019	0.3355	0.0255	0.0025	1751.68	0.0520

Appendix VIII: Table of Water-Side Properties

Hot Exchanger Results

Data Point	water properties					
	mu	mu(s)	density	cp	k	Pr
1	0.000983		998.20	4181.60	0.60	6.81
2	0.000983		998.20	4181.60	0.60	6.81
3	0.000983		998.20	4181.60	0.60	6.81

Cold Exchanger Properties

Data Point	water properties					
	mu	mu(s)	density	cp	k	Pr
1	0.000983		998.20	4181.60	0.60	6.81
2	0.000983		998.20	4181.60	0.60	6.81

51

Appendix IX: Thermoacoustic Sample Calculation

This sample calculation is based on the first data point listed in the first four appendices for the microchannel rejection heat exchanger. If there is any small difference caused by round-off error, the correct value will be listed.

- Using the measured data from Appendix I, construct a DeltaE model to predict the particle velocity in each heat exchanger.

  - $u = 2.9407$ m/s

- Take the velocity found from DeltaE and find the rms velocity by dividing by $\sqrt{2}$.

  - $u_{rms} = \dfrac{u}{\sqrt{2}} = \dfrac{2.9407}{\sqrt{2}} = 2.0794$ m/s

- Find the hydraulic diameter

  - Find the flow area(A_c)

$$A_c = \pi R^2 - tL - w_t L_t$$
$$= \pi \times 0.0762^2 - 0.0001016 \times 12.272038 - 0.0018288 \times 2.143235966$$
$$= 0.01307508 \text{ m}^2$$

  - Find the total heat exchanger surface area(A)

$$A = A_f + A_t = L_t \times 2(w_t + t_t) + L \times 2(w + t)$$
$$= 2.143235966 \times 2(0.0018288 + 0.005969) + 12.272038 \times 2(0.0079375 + 0.0001016)$$
$$= 0.230737332 \text{ m}^2$$

  - $D_h = \dfrac{4LA_c}{A} = \dfrac{4 \times 0.0079375 \times 0.01307508}{0.230737332} \cong 0.0018 \text{ m}$

- Find the Reynolds number

  - $\text{Re} = \dfrac{u_{rms}\rho D_h}{\mu} = \dfrac{2.0794 * 11.029 * .0018}{.000024} = 1727.93$

52

- Find the log mean temperature difference as the difference between the stack end temperature and the water inlet temperature.

  - $$LMTD = \frac{(T_{w,o} - T_{w,i})}{Ln\left\{\dfrac{T_s - T_{w,i}}{T_s - T_{w,o}}\right\}} = \frac{.88}{Ln\left\{\dfrac{-3.49}{-2.61}\right\}} = 3.03\,\text{K}$$

- Find UA by dividing the hot heat exchanger power by the LMTD

  - $$UA = \frac{Q_h}{LMTD} = \frac{175.1}{3.03} = 57.84$$

- Use the definition of UA (Equation 6) to solve for h_o. Unfortunately, the hyperbolic tangent in the efficiency makes it impossible to explicitly solve for h_o. Thus, it must be solved iteratively.

  - $$UA = \frac{1}{\dfrac{1}{\eta_o h_o A_o} + R_{tw} + \dfrac{1}{h_i A_i}} = \frac{1}{\dfrac{1}{.7799*h_o*.231} + 6.387E-5 + \dfrac{1}{3737.01*.02646}} = 57.84$$

  where

  - $$\eta_o = 1 - \frac{A_f}{A}(1 - \eta_f) = 1 - \frac{.1973}{.2307}(1 - .7426) = .7799$$

  - $$\eta_f = \frac{\tanh(mL)}{mL} = \frac{\tanh(286.1*.0037)}{286.1*.0037} = .7426$$

  - $$m = \sqrt{\frac{Ph_o}{kA_c}} = \frac{.01608*h_o}{190.4*8.065E-7} = 286.1 \text{ m}^{-1}$$

  - $$R_{tw} = \frac{\ln(D_o/D_i)}{2\pi L_{tube}\,k_t} = 6.387E-5 \text{ K/W}$$

  with the iterative solution of

  - $$h_o = 781.6 \text{ W/m}^2\text{-K}$$